Helsinki University of Technology Radio Laboratory Publications
Teknillisen korkeakoulun Radiolaboratorion julkaisuja
Espoo, August 2005 REPORT S 272

DESIGN OF HIGH-EFFICIENCY ANTENNAS FOR MOBILE COMMUNICATIONS DEVICES

Outi Kivekäs (née Lehmus)

Dissertation for the degree of Doctor of Science in Technology to be presented with due permission for public examination and debate in Auditorium S4 at Helsinki University of Technology (Espoo, Finland) on the 19th of August 2005 at 12 o'clock noon.

Helsinki University of Technology
Department of Electrical and Communications Engineering
Radio Laboratory

Teknillinen korkeakoulu
Sähkö- ja tietoliikennetekniikan osasto
Radiolaboratorio

Distribution:
Helsinki University of Technology
Radio Laboratory
P.O. Box 3000
FI-02015 TKK
Tel. +358-9-451 2252
Fax. +358-9-451 2152

ISBN 951-22-7756-5
http://lib.tkk.fi/Diss/
951-22-7758-1

ISSN 1456-3835

Otamedia Oy
Espoo 2005

Preface

The work for this thesis has been done at the Radio Laboratory of Helsinki University of Technology during 1999-2004. Part of the work has been done in projects funded by the National Technology Agency of Finland (TEKES), Nokia Mobile Phones, Nokia Research Center, and Filtronic LK. The work has also been funded partly by the Graduate School in Electronics, Telecommunications, and Automation (GETA) and partly by the Academy of Finland. In addition, Nokia Foundation, Jenny and Antti Wihuri Foundation, Emil Aaltonen Foundation, the Finnish Society of Electronics Engineers, and HPY Foundation have financially supported my postgraduate studies. I am grateful for all the financial support I have received during the work.

I am deeply thankful to my supervisor Prof. Pertti Vainikainen for the opportunity to work in interesting industrial and academic projects. Particularly, I want to thank him for his encouraging guidance and active participating into my studies - his numerous ideas have been essential for this thesis. I am also grateful to him for the possibility of doing some of my research work at home.

Two experts in the field, Prof. Michal Okoniewski and Dr. Anssi Toropainen, were the preliminary examiners of this thesis. I wish to express my sincere gratitude to them for reviewing my thesis and for their valuable comments and suggestions regarding the manuscript.

I am thankful to Dr. Jani Ollikainen for being a creative instructor throughout my post-graduate studies. His contribution to this thesis has been invaluable. Also, I want to thank him for sharing the joys and pains of research over these years as well as for good companionship. In addition, I thank Tuukka Lehtiniemi and Milla Mikkola for all their help and important input in the *SAR* studies. I also highly appreciate the fruitful cooperation in several research projects I have participated during these years, and I thank all the participants; it has been a pleasure to work with you. Especially, I want to acknowledge Joonas Krogerus for his help.

I wish to thank the present and former personnel of the Radio Laboratory for the memorable years in the lab. Especially, I thank Dr. Kati Sulonen for sharing the every-day life in the same room for several years and for friendship. Also, I want to express many thanks to secretaries Stina Lindberg and Tuula Mylläri for their readiness to help in various matters and pleasant company; to Dr. Jaakko Juntunen for good cooperation with DRAs; to Dr. Clemens Icheln for his help with many practical issues and especially with the computers; and to Janne Häkli and Pasi Suvikunnas for interesting discussions on everything and beyond. In addition, I thank Marja Leppäharju from GETA for her always glad and supporting attitude.

“The Girls”, Kaisa, Heidi, Heli, Outi, Päivi, Suvi, and Tiina, deserve special thanks for friendship and many good moments spent together without antenna issues.

I am thankful to my parents Airi and Heikki and to my sister Päivi for their encouragement during the whole course of my studies. Warm thanks belong to my Mum also for babysitting. My dearest thanks are to my husband Kalle for being the greatest support of all and to our daughters Anna and Emilia for giving me so much joy. Without my family’s love and understanding this work had never been finished.

Espoo, June 12, 2005

Outi Kivekäs

Abstract

This thesis deals with the design of high-efficiency antennas for small mobile communications devices. Owing to the continuously stricter requirements set for multisystem mobile terminals, the ongoing need for efficient antennas in personal mobile communications is evident. In this work, the entire system consisting of the antenna; the mobile terminal working actually as part of the antenna; and the user of the terminal is considered. The ratio between the power radiated into the free space and the antenna input power, i.e. the total efficiency of this system, forms a general concept for the studies. The total efficiency is partly affected by the losses in the antenna element. As the antenna efficiency, bandwidth, and volume are strongly interrelated exchangeable quantities, it is essential to find other approaches for enhancing the antenna efficiency than simply sacrificing other performance. Further, the metal chassis of a mobile terminal has to be part of the antenna element design because of its considerable effect on antenna performance. In addition, the total efficiency of the entire system is partly affected by the losses owing to the user. Thus, the evaluation of antenna performance is equally important when the mobile terminal is located near a user or when it is in free space. The main goal of this work is to provide novel and useful information for the design of mobile terminal antennas with special emphasis placed on the maximization of the total efficiency.

To obtain necessary background understanding for the design of antennas with minimized user interaction, the general energy-absorption mechanism in the human tissue is studied in this thesis. It is shown that the peak *SAR* (specific absorption rate) is not actually related to the antenna current, as has been commonly believed. Instead, the *SAR* maximums can be explained by inspecting the antenna's quasi-static electric near field components perpendicular and parallel to the surface of the tissue at the air-tissue interface and utilizing the boundary conditions of quasi-static fields at the interface. As *SAR* is directly proportional to the total electric field in the tissue, the *SAR* distributions caused by a certain antenna differ considerably in tissues with different permittivity values, e.g. brain and fat.

The bandwidth, efficiency in talk position, and *SAR* performance of a typical monoblock handset antenna-chassis combination is comprehensively investigated in this work for clarifying the roles of different parts of the radiating system. The system is treated as a combination of the separate wavemodes of the antenna element and the chassis. Based on the results, guidelines are given to control or analyze the combined performance both in the sense of radiation properties (bandwidth, efficiency) and user interaction (*SAR*). It is also demonstrated that there is a connection between the studied three performance parameters: a local maximum in *SAR* values and a local minimum in radiation efficiency occur when the bandwidth reaches its maximum and the resonant frequency of the chassis equals that of the antenna.

The suitability of dielectric resonator antennas (DRA) for mobile terminals is studied theoretically and experimentally with the main attention paid to the loss characteristics. It is observed that DRAs are appropriate for this purpose especially when very small antenna elements are needed. As an application example, a novel means to realize a high-performance dual-resonant antenna design for mobile terminals is presented.

In addition, losses in the frequency-tuning circuits of small resonant antennas are systematically investigated. Design guidelines for tuning circuits with minimized losses with respect to the achievable tuning range are given. Based on the proposed theory, a low-loss tuning circuit with suitable characteristics for mobile terminal antennas is introduced.

Table of contents

List of publications

This thesis is based on the work presented in the following papers:

P1 O. Kivekäs, T. Lehtiniemi, and P. Vainikainen, ”On the general energy-absorption mechanism in the human tissue,” *Microwave and Optical Technology Letters*, vol. 43, no. 3, Nov. 2004, pp. 195-201.

P2 P. Vainikainen, J. Ollikainen, O. Kivekäs, and I. Kelander, ”Resonator-based analysis of the combination of mobile handset antenna and chassis,” *IEEE Transactions on Antennas and Propagation*, vol. 50, no. 10, Oct. 2002, pp. 1433-1444.

P3 O. Kivekäs, J. Ollikainen, T. Lehtiniemi, and P. Vainikainen, “Bandwidth, *SAR*, and efficiency of internal mobile phone antennas,” *IEEE Transactions on Electromagnetic Compatibility*, vol. 46, no. 1, Feb. 2004, pp. 71-86.

P4 O. Lehmus, J. Ollikainen, and P. Vainikainen, ”Characteristics of half-volume DRAs with different permittivities,” *IEEE Antennas and Propagation International Symposium Digest (AP-S 1999)*, vol. 1, Orlando, FL, July 11-16, 1999, pp. 22-25.

P5 O. Kivekäs, J. Ollikainen, and P. Vainikainen, ”Wideband dielectric resonator antenna for mobile phones,” *Microwave and Optical Technology Letters*, vol. 36, no. 1, Jan. 2003, pp. 25-26.

P6 J. Ollikainen, O. Kivekäs, and P. Vainikainen, “Low-loss tuning circuits for frequency-tunable small resonant antennas,” *Proc. 13th IEEE International Symposium on Personal, Indoor, and Mobile Radio Communications (PIMRC 2002)*, Lisbon, Portugal, Sept. 15-18, 2002, pp. 1882-1887.

P7 O. Kivekäs, J. Ollikainen, and P. Vainikainen, “Frequency-tunable internal antenna for mobile phones,” *Proc. 12th International Symposium on Antennas (JINA 2002)*, vol. 2, Nice, France, Nov. 12-14, 2002, pp. 53-56.

Other related papers authored or co-authored by the author of this thesis are given in the reference list as [O1]-[O15].

Contributions of the author

As a general guideline, the first author of each paper had the main responsibility for the manuscript. Professor Pertti Vainikainen supervised all the papers.

The simulations of paper **P1** were performed in co-operation with Tuukka Lehtiniemi, but the author of this thesis had the main responsibility for those. Tuukka Lehtiniemi also assisted in data processing. The analysis of the results was done together with this author and Pertti Vainikainen.

In paper **P2**, this author had the main responsibility for the part that deals with specific absorption rate and radiation efficiency. In addition, this author participated in preparing the manuscript.

In paper **P3**, this author had the main responsibility for the simulations concerning *SAR* and efficiency and for the analysis of the results. This author also performed the measurements. Jani Ollikainen had the main responsibility for the bandwidth considerations. He also contributed to the *SAR* and efficiency simulations and the analysis of the results. Tuukka Lehtiniemi assisted in data processing and with the prototypes.

In paper **P4**, this author carried out the design, measurements, and analysis of the reported antennas. Jani Ollikainen participated in the work as an instructor.

The antenna structure presented in **P5** is a joint invention of the authors and Jaakko Juntunen. The prototype was designed together with this author and Jani Ollikainen. This author had the main responsibilities for the theoretical studies, the measurements of the antenna, as well as the analysis of the results.

In paper **P6**, this author participated in the theoretical calculations. The measurements were performed in co-operation with Jani Ollikainen, who had the main responsibility for those and for the prototype antennas as well. In addition, this author participated in the writing of the paper.

Paper **P7** is based on the idea of this author and Jani Ollikainen. This author had the main responsibility for the design, construction, and measurement of the antenna as well as the analysis of the results.

1 Introduction

1.1 Background

The evolution of personal communications systems has increased the need for the development of small antennas for mobile terminals. Currently, the tendency in wireless communications is in universal multisystem terminals: modern mobile handsets need to operate in various systems and thus in several frequency bands. It is necessary to have a high-performance antenna for each system. Some of the systems will also require the use of diversity antennas. In these respects, the number of antennas in a mobile terminal will increase.

For some time, the main trend has been in internal antenna elements instead of external whip and helix antennas used previously in handsets. As there is a limited space for antennas inside the casing of a terminal, antennas with as small size as possible are needed. One great challenge in the antenna development is to realize compact antenna elements with sufficient bandwidth and high efficiency, as there is a strong interrelation between the antenna volume, bandwidth, and efficiency. It is not reasonable to simply improve one property while trading off another. Instead, alternative methods have to be found. Besides, universal antenna elements cannot be realized because the antenna performance depends strongly on the size of the metal parts of the device onto which the antenna is mounted (chassis) and the location of the antenna on it. The antenna couples currents on the chassis, and the device itself works as part of the antenna. Actually, the user of a mobile terminal is also a part of the radiating system, as the nearby human tissue affects the electromagnetic fields of the device. Thus, the entire mobile communications device and its user have to be part of the antenna design.

The ongoing need for further antenna development originates from several aspects, one being the continuously stricter requirements, e.g. bandwidth-to-volume ratio, set for antennas in multisystem mobile terminals, another being the radio frequency (RF) exposure limits, which all mobile terminal devices must meet in all conditions. The reduction of the absorption of RF power from mobile terminal antennas by the users will also make the antenna more efficient, which is another important reason for investigations on mobile terminals in the vicinity of a user. Owing to the limited energy available, a handset antenna has also to have as high free space efficiency as possible. A high-efficiency antenna leads to technical advantages, such as lower power consumption, and thus a longer standby and talk time of the phone.

1.2 Objectives of the work

In this thesis, the entire system including the antenna; the mobile terminal being an important part of the antenna; and the user of the terminal is considered. The main emphasis is put on the maximization of the total efficiency of this system. This can be defined as the ratio between the power radiated into the free space and the antenna input power. The ratio is affected partly by the losses in the antenna element, partly by the losses in other mobile terminal parts, such as the plastics, battery, and display, and partly by the losses owing to the user. The studies of this thesis are limited to antenna element and user losses.

The general objective of this work is to provide novel and useful information for the design of mobile terminal antennas. One of the main purposes is to improve the understanding of the basic energy-absorption mechanism in the human tissue, as the earlier knowledge on this issue seems to be somewhat unclear. Another important purpose is to comprehensively investigate the combined performance of a small antenna and chassis, because the effect of the mobile terminal chassis on the

antenna performance is known to be significant, but the existing analysis is inadequate. In this work, special attention is paid to the user interaction of an antenna-chassis combination. A further aim is to study new approaches for realizing efficient mobile terminal antennas with compact size and sufficient bandwidth.

1.3 Contents of the thesis

This thesis is divided into two parts. In the first part, an overview of the main design issues for mobile terminal antennas is presented including considerations for both the antenna element and the antenna-chassis combination. In addition, this part includes a discussion on the basic energy-absorption mechanism; and short descriptions of dielectric resonator antennas and of the frequency-tuning of small resonant antennas. The first part also forms a summary of the work, which is given to introduce the background of the actual scientific work presented in the enclosed papers [P1]-[P7] forming the second part of this thesis. In [P1], the general energy-absorption mechanism is discussed. The combination of a mobile handset antenna and chassis is studied theoretically and experimentally in [P2], and its bandwidth, specific absorption rate (*SAR*), and efficiency performance is further analyzed in [P3]. Paper [P4] describes the general characteristics of half-volume rectangular DRAs, and paper [P5] presents a wideband DRA application for mobile terminals. A design method for frequency-tunable antennas is proposed in [P6]. Based on the theory of [P6], a practical frequency-tuning circuit for mobile handset antennas is introduced in [P7] to demonstrate a handset application.

2 Main requirements for mobile terminal antennas

Antenna elements of mobile terminals can be defined as small antennas. A common definition for a small antenna is that its greatest dimension is limited to be smaller than $\lambda_0/4$ including any image due to ground plane [1]. Here, λ_0 is the free space wavelength. Resonator theory can be applied to small antennas, as near its fundamental resonance, any small antenna can be approximated as a resonant circuit, where a feed arrangement is added. A small antenna is not always in itself resonant, in which case a matching circuitry is added to achieve resonance.

In this chapter, the general requirements for small antennas in wireless mobile terminals are briefly presented to be able to understand the basic challenges and limitations in antenna design. At present, microstrip-type antennas are most commonly used in handsets. Therefore, most examples in this chapter refer to this antenna type. However, the presented requirements apply to all types of antennas in wireless mobile terminals. The primary requirements concern the volume occupied by the antenna element and the electrical performance with bandwidth, efficiency, and specific absorption rate as the most significant parameters. Only the most important performance requirements are discussed here leaving out the essential requirements for antennas in commercial products, such as fabrication considerations and antenna cost. In addition, the effect of the terminal chassis, which is significant from the basic operation point of view, is excluded from this chapter. However, that issue is comprehensively considered in Chapter 4.

2.1 Size

In a mobile handset, there is only a limited space provided for an antenna. Thus, handset antennas are required to be small in volume. A convenient shape of a mobile casing calls for low-profile antenna structures. In general, the aim is a small-size broadband effective antenna. However, the antenna dimensions cannot be diminished endlessly without antenna performance being affected, as will be discussed in the next section. Hence, designing small antennas is always a trade-off between the antenna size, bandwidth, and efficiency.

2.1.1 Fundamental limitations on size reduction

An antenna element couples to a free space wave, which has a settled wavelength value depending simply on the operating frequency. This forms the basis for the limitations on small antenna size reduction. The main studies of the fundamental limits and antenna performance have been published already tens of years ago [1], [2], [3], [4], [5], [6], [7]. They show that the impedance matching of a small antenna can be achieved efficiently only over a narrow bandwidth. The smaller the antenna size relative to the wavelength is, the narrower the achievable bandwidth becomes. When reducing the antenna size, the radiated power also decreases in comparison to the ohmic losses. This decreases the antenna efficiency.

The equation for the minimum theoretical radiation quality factor Q_r is derived by assuming the entire antenna completely enclosed within a sphere of radius r. Q_r is calculated in terms of the nonpropagating energy external to the sphere and the radiated power. This approach was first introduced in [3]. For the lowest order wavemode in a linearly polarized antenna the radiation quality factor becomes [8]:

$$Q_r = \frac{1}{(kr)^3} + \frac{1}{kr}, \qquad (2\text{-}1)$$

where $k = 2\pi/\lambda_0$ is wave number and r is the radius of the smallest sphere enclosing the antenna.

Eq. (2-1) can be referred to as the fundamental limit, as to how small an antenna can be made. According to this equation, Q_r grows rapidly when the antenna size decreases, as Q_r is approximately inversely proportional to the volume of the antenna in wavelengths (V/λ_0^3). When the sphere containing the antenna element becomes very small, no propagating modes exist, because all modes are below cutoff frequency. Fundamental limit on the electrical size of the antenna can be approached but never reached or exceeded. In practice, antennas do not completely make use of the spherical volume. In addition, also other wavemodes are excited than just the lowest ones. These additional modes, as well as the lowest order modes, always store energy also within the enclosing sphere; this inevitably increases the Q_r [5]. In [9], it is studied how reachable the theoretical limit is with real antennas. A spherical helix antenna with four wires, which quite effectively utilizes the spherical volume, gives a reference point for compactness. The ratio between the calculated radiation quality factor and the theoretical one is 1.25. For more practical antennas, the calculated results stay further from the theoretical ones, e.g. for a small dipole (length/wavelength = 0.2) $Q_r / Q_{r,\,theory} = 9.17$ [9]. However, the dipole utilizes poorly the available volume.

2.1.2 Miniaturization

When competently miniaturizing an antenna, the resonant frequency remains the same even though the antenna size is reduced. Actually, miniaturizing can also be considered as a decrease in the resonant frequency while preserving the antenna size. There are several means for miniaturization. Typically downsizing can be accomplished:

- by appropriately placing a metallic plane into an antenna system, and then utilizing image theory to remove half of the antenna structure.
- by loading the antenna in a way that the self-resonance is obtained when the antenna volume is smaller than that of a basic structure. The antenna can be loaded dielectrically or reactively.
- by increasing the effective resonator length by bending the structure according to some geometrical configuration, e.g. meandering.

Several techniques can be applied simultaneously to further reduce the antenna size. However, there are no means for downsizing an antenna without sacrificing the performance. Thus, the interrelation between the bandwidth, volume, and efficiency cannot be avoided, but the trade-off contributions can be affected by applying different miniaturization methods. This issue has been studied in [10].

2.2 Bandwidth

When dealing with small antennas, the term bandwidth typically refers to the impedance bandwidth. A handset antenna should have an adequate bandwidth covering the frequency range used by a certain wireless communication system. The detailed requirements for operating frequency and bandwidth are different for each system. Typically, the goal for the impedance bandwidth in cellular systems could be defined as the return loss of $L_{retn} \geq 6$ dB for the whole operating frequency range. This means that up to 25 % of the total input power is lost due to the mismatch. Bandwidth is typically measured in free space, and owing to the dielectric loading, it is somewhat different from that in a typical handset use position in the vicinity of a user [11], [12], [13], [14].

2.2.1 Multiband antennas

Current and future mobile terminals operate in various communications systems. Therefore, multiband antennas, which have several bands of operation, are needed. Sufficient performance in all bands is essential. In microstrip-type antennas the multiband operation is typically implemented by dividing the antenna element into two or more patches, which each have different resonant frequencies and operate in different systems, e.g. [15], [16], [17], [18]. Resonant slots can also be utilized in multiband antennas [19]. Recently, dual-band dielectric resonator antennas have been realized by inserting an air slit into the dielectric resonator [20], merging the resonance of an aperture feed and a DRA [21], or adding a parasitically coupled conducting strip to the structure [22].

2.2.2 Multiresonant antennas

Because of the problematic nature of small antennas concerning the interrelation between the antenna size, bandwidth, and efficiency, there is no complete freedom to independently optimize each property. Consequently, there is a need for bandwidth enhancement techniques. With a fixed size and efficiency, one way to increase the bandwidth is to add more resonators into the structure. Multiresonant antenna has several resonances tuned close to each other to obtain a wider bandwidth. In [23], it has been demonstrated that the bandwidth of a single-resonant antenna can be more than doubled with a dual-resonant antenna structure of equal size. Multiple resonances can be realized by using parasitic radiating elements [24], [25], [26] or resonant matching circuits [O9], [27]. Multiresonant antennas have also been studied in this thesis. In [P5], a dual-resonant dielectric resonator antenna, which is fed by a self-resonant meandered probe, is proposed (see Section 5.2). In [P7], a frequency-tunable antenna utilizing dual resonance is presented (see Section 6.2). A multiresonant antenna can also be utilized when implementing a multiband antenna, e.g. [O2], [28].

2.2.3 Frequency-tunable antennas

Another feasible technique to improve the effective bandwidth of a small antenna is to electrically tune its resonant frequency, and thus its operation band [29], [30]. This can be realized by loading the antenna with a reactive tuning component. Frequency band can be tuned within a system band or between bands of different communication systems. Therefore, frequency-tunable antennas do not necessarily cover the whole system band or many system bands simultaneously, but they provide narrow instantaneous bands. The advantages are the reduced total antenna volume or the reduced number of antennas, and the increased selectivity. However, the tuning circuit unavoidably increases the component count and decreases the efficiency [31], [32]. In addition, distortion caused by the non-linearity of the tuning components can also be a problem [33], [34]. Frequency-tunable antennas will be further discussed in Chapter 6.

2.3 Efficiency

Radiation efficiency, which characterizes the losses in the antenna, is defined as the ratio of the radiated power to the input power of the antenna. Radiation efficiency does not take into account the losses due to mismatch at the antenna input. Thus, L_{retn} = 6 dB at the edges of the operating band means a 1.26 dB additional loss caused by the reflection. Total efficiency of an antenna is defined as the ratio of the radiated power to the power accepted by the antenna; therefore, it also includes the effect of imperfect matching.

The efficiency of handset antennas should be as high as possible. This leads to technical advantages, such as lower power consumption, and thus a longer standby and talk time of the phone. In this thesis, maximization of the antenna efficiency is emphasized.

2.3.1 Efficiency in free space

In a good design, the value for the free space radiation efficiency of a mobile handset prototype including only antenna and metal chassis is approximately above 90 % over the operating frequency band. It means that less than 0.5 dB is lost in the structure. In most publications, the information on radiation efficiency is not available – in particular not for the whole band. Designs with relatively high free space radiation efficiency values (approximately 1 dB loss at maximum, i.e. minimum radiation efficiency of about 80 %) over the whole operating bands are described e.g. in [O2], [O9], [O12], [28]. In these cases, the power is mainly lost in imperfect conductors, as the antenna structures do not contain any additional components, e.g. switches, which increase the total losses [31]. In real mobile terminals, the radiated power is partly lost in mobile phone parts, e.g. battery, display, and plastics. Free space radiation efficiencies of commercial dualband phones were studied by measurements in [35] and [36]. Values of 54-80 % and 32-72 % averaged over the GSM900 (880-960 MHz) and GSM1800 (1710-1880 MHz) bands, respectively, were reported.

2.3.2 Efficiency beside user

A mobile terminal is located in very close proximity to the user in a typical operating situation. When RF radiation is emitted from a mobile terminal held next to a human, a portion is radiated away into the surrounding air, and body tissues absorb another portion. When a mobile terminal is located in a traditional talk position, mostly head and hand regions absorb RF radiation. The situation is different when a mobile terminal is located in some body-worn position, e.g. when it is in a pocket near the user's body.

Depending on the design, the human head absorption may be 1.5-10 dB [37]. Variations are large owing to e.g. different antenna types [12], [13], [38]; different chassis parameters (this issue is studied extensively in this thesis, see Section 4.3); different operating frequencies [14], [39]; different phone positioning; and different simulation and measurement models used in the studies. Diverse values are also reported for the absorption by hand. For example, very low hand absorption (< 0.2 dB) has been reported in [11] for a handset with monopole antenna at 914 MHz, whereas 4-5 times larger absorption was shown in a corresponding case in [12]. Typically, larger power absorption in hand is reported with phones having a patch antenna than with phones having a monopole antenna [12], [40]. In addition, the varying hand positions have been shown to radically affect the hand absorption [41]. Even very small variations in the way the handset is held may affect the hand loss significantly, e.g. in [41], the hand loss of approximately 2 dB is reported for a handset with patch antenna at 1800 MHz, while moving the index finger increases the hand loss by additional 2.8 dB.

2.4 Specific absorption rate (*SAR*)

Regulatory agencies have set mandatory safety guidelines for RF exposure, which a mobile phone has to fulfill (see Section 2.4.1). The primary dosimetric parameter for the evaluation is the specific absorption rate. Therefore, *SAR* is an important design specification of a mobile terminal antenna. It is a measure to quantify the microwave energy absorbed by unit mass of tissue and defined as

$$SAR = \sigma_{eff} \frac{E^2}{\rho}, \tag{2-2}$$

where σ_{eff} is the effective conductivity of the tissue (S/m), E is the root-mean-square (rms) value of the induced electric field strength (V/m), and ρ is the tissue mass density (kg/m^3). The *SAR* value is expressed in units of watts per kilogram (W/kg), and it denotes the time rate of RF energy absorption at a given location inside the tissue.

There are two general approaches to the determination of the *SAR* in the human tissue: experimental and numerical techniques. Both physical measurement and numerical simulation methods to evaluate *SAR* have been studied intensively. Representative descriptions on measurement setups and methods are given in [42], [43], [44] and on numerical dosimetry in [45].

2.4.1 Limitations and specifications

Several regulatory bodies have set safety limits for the *SAR* values caused by a phone, e.g. [46], [47]. The most widely accepted RF exposure recommendations are based on guidelines developed by the Institute of Electrical and Electronics Engineers and American National Standards Institute (IEEE/ANSI) [48] and the International Commission on Non-Ionizing Radiation Protection (ICNIRP) [49], which is an independent scientific organization sponsored by World Health Organization (WHO). The *SAR* limits are provided to prevent whole-body heat-stress and excessive localized tissue heating. The major RF exposure recommendations have been developed by identifying the adverse effect of RF exposure that has been found in animals at the lowest exposure level. There is a general agreement with energy absorption of 4 W/kg of body weight being the threshold rate for the induction of biological thermal effects. When exposed to this amount of RF energy, an animal stops performing a task and begins a different behavior resulting from excessive body heating. With safety factors of 50 and 10, the human whole body exposure has been limited to 0.08 and 0.4 W/kg for uncontrolled and controlled environments, respectively. In an uncontrolled environment, a person is unaware of the exposure (general public exposure), such as a mobile phone user, and in a controlled environment, a person is aware of the exposure (occupational exposure). When the power absorption occurs in confined body regions, as in the case of the head or hand exposed to a mobile phone, the local *SAR* may have rather high values even if the average whole body *SAR* is below the basic limit. The restrictions for partial body exposure are based on different rationales, e.g. the IEEE/ANSI limits are based on the maximum approximate ratio of the peak *SAR* at one point to the *SAR* averaged over the whole body (20:1) [48], and the ICNIRP guidelines have their basis on animal studies [49]. However, no biological significance should be associated with these slight differences. The main parameters of the most important safety guidelines from the handset antenna design point of view are listed in Table 2.1.

Table 2.1 *Basic RF exposure restrictions in an uncontrolled environment (general population) set by IEEE/ANSI and ICNIRP.*

	IEEE/ANSI	**ICNIRP**
Whole body averaged SAR (W/kg)	0.08	0.08
Spatial peak SAR (W/kg) in body except hands, wrists, feet, ankles	1.6	2
Averaging mass (g)	1	10
Volume shape	Cube	Any of 10 g contiguous tissue
Spatial peak SAR (W/kg) in hands, wrists, feet, ankles	4	4
Averaging mass (g)	10	10
Volume shape	Cube	Any of 10 g contiguous tissue
Averaging time (min)	30	6

3 General energy-absorption mechanism

When microwaves propagate in a dielectric material, such as human tissue, the generated internal electric field induces transitional motions of charged particles and rotates charge complexes. Mainly frictional forces resist these induced motions and cause losses, which result in absorption of energy [50]. Thus, it is well-known how the internal electric fields interact with material. However, the rationale behind the connection between the originally applied external fields and the generated internal fields, and therefore the resulting *SAR* values, i.e. a relevant part of the general energy-absorption mechanism, has not been fully explained. Nevertheless, this is an important topic from the efficiency point of view, as in general, all the power that is not induced into the user of a mobile terminal radiates into the free space. Therefore, minimizing the user interaction (*SAR*) improves the total efficiency of a mobile terminal. The basis of the energy-absorption mechanism is considered in this chapter.

A principal, often-referred-to paper [51] studies the general energy-absorption mechanism in the close near field of dipole antennas operating above 300 MHz. One goal of this study was to find a simple approximation for the relation between the fields of a dipole-like source and the corresponding worst-case exposure *SAR* values. Thus, the starting point was to study magnetic fields, as electric fields undergo structural changes in the presence of dielectric bodies, whereas the antenna current distribution is less affected. The *SAR* in the human tissue was shown to be mainly proportional to the square of the incident magnetic field strength at the skin surface of the user. Therefore, it was concluded that the major interaction mechanism is based on the surface currents induced by the magnetic fields, and the coupling of the electric fields is of minor importance [51], [43]. As a result, an approximate formula for the spatial peak *SAR* caused by a nearby half-wavelength dipole antenna was written as a function of antenna feedpoint current and human tissue parameters.

On the other hand, the conclusion drawn on the base of the main interaction mechanism in [51] is not supported by the results of [52], in which numerical computation of fat layer effects on the microwave near field radiation was presented. A dipole at 915 MHz was located beside a homogeneous muscle phantom with and without a fat layer covering the abdomen. It was found that without a fat layer, the *SAR* pattern was elliptical around the antenna feed point, which confirms the results of [51]. However, with 0.8 and 1.6 cm thick fat layers on the muscle surface, two *SAR* hot spots were observed on the fat surface near the ends of the dipole. No reason for the different locations of *SAR* maximums in the muscle or in the fat layer was provided in the paper. It was also shown that the peak *SAR*, average *SAR* and total power absorbed by the body with a fat layer were much lower than those without a fat layer, as fatty tissues do not absorb RF power strongly due to their material properties (low ε_r' and σ_{eff}). Thus, it was reported that especially a thick fat layer behaves like a shielding structure for the muscle tissue preventing microwave absorption in the muscle. However, the thick fat layer also increases the distance between the antenna and the muscle, and this obviously decreases the power absorption in the muscle as well.

Due to these rather controversial results, the electromagnetic absorption mechanism in the human tissue seemed to be an issue, which had long been, to some extent, somewhat unclear. The topic was investigated further in [P1], in which the behavior of the electric fields of small antennas located near lossy dielectric half-space was studied by numerical simulations. The paper is limited to the study of the electric fields utilizing the basics of the perturbation theory. Generally, the perturbation theory is used to describe the interaction between the fields of an electromagnetic resonator and materials inserted into it. The electromagnetic field perturbation of a resonant cavity by a small sample inserted in it is a common method for defining the properties of low-loss materials. This requires determining the shift of the cavity resonant angular frequency from the original unperturbed value to a new perturbed value. The change in the imaginary part of the resonant angular frequency can be interpreted

as the change in the loaded quality factor of the resonator, and therefore the loss mechanisms for the interaction can be defined. The general perturbation formula, which applies to a change in magnetic permeability (μ) as well as to a change in permittivity, is [53]:

$$\frac{\omega_{r2}-\omega_{r1}}{\omega_{r2}} = -\frac{\int_V \left[(\varepsilon_{r2}-\varepsilon_{r1})\varepsilon_0 \vec{E}_2 \cdot \vec{E}_1^* + (\mu_{r2}-\mu_{r1})\mu_0 \vec{H}_2 \cdot \vec{H}_1^*\right] dV}{\int_V \left[\varepsilon_{r1}\varepsilon_0 \vec{E}_2 \cdot \vec{E}_1^* + \mu_{r1}\mu_0 \vec{H}_2 \cdot \vec{H}_1^*\right] dV}, \qquad (3\text{-}1)$$

where ω_r is the angular resonant frequency, ε_r is the relative permittivity, ε_0 is the permittivity in vacuum, $\vec{E}$ is the electric field strength, μ_r is the relative permeability, μ_0 is the permeability in vacuum, and $\vec{H}$ is the magnetic field strength. The subscript 1 refers to the situation before the insertion of the sample, and the subscript 2 refers to the situation after the change. Though normally applied for small perturbations, the equation for the effect of materials on the resonant frequency is actually valid also for cases, where the dielectric object fills a significant part of the effective volume of the resonator [54], like in the studied problem.

In Eq. (3-1), the magnetic field term in the numerator disappears when the permeability is unchanged ($\mu_{r1} = \mu_{r2}$), as is the case where we deal with non-magnetic materials. The denominator describes the total energy in the resonator. At resonance, the stored electric energy equals the magnetic energy, and the denominator can be substituted by twice the value of the first term in the integral. Therefore, when considering static fields in low-conductivity non-magnetic materials, such as human tissue, the magnetic fields are insignificant, and the analysis of just the electric fields is justifiable.

The results of [P1] show that contrary to the previous opinion, the *SAR* maximum does not actually follow the maximum of the antenna current. Instead, the *SAR* maximums can be explained by the general laws of the interaction of electromagnetic fields and matter by inspecting the real part of the permittivity of the tissue and its effect on the electric field components perpendicular and parallel to the surface of the tissue. This is illustrated in Figure 3.1. Figure 3.1a illustrates the simulation geometry. A more detailed description of the simulation models is given in [P1]. Figures 3.1b-d show the normalized E_x (perpendicular to the dielectric surface) and E_z (parallel to the dielectric surface) for a dipole in free space and when a dielectric half-space is located at $x \le 0$ mm. The E_y-components are so weak (below –120 dB), that they are not shown. In Figure 3.1b, the whole dielectric half-space consists of tissue-equivalent liquid (TEL, $\varepsilon_r' = 42.50$), whose material properties are those used for *SAR* compliance testing. In Figure 3.1c, an 8 mm-thick bone layer ($\varepsilon_r' = 16.62$) and on top of that a 7 mm-thick muscle layer ($\varepsilon_r' = 55.95$) cover the TEL surface. In Figure 3.1d, a 7 mm-thick fat layer ($\varepsilon_r' = 5.00$) covers the TEL surface. The plotted curves are from the center of a *z*-directed dipole ($z \approx 0$ mm).

It can be noted from Figures 3.1b-c that for high values of the real part of permittivity, such as tissue-equivalent liquid or muscle, the perpendicular electric field component (E_x) is attenuated substantially at the surface. In the case of fat layer, which has much lower real part of permittivity, the corresponding component attenuates much less. The theoretical approximation for E_x is obtained based on boundary conditions by dividing the perpendicular component in free space by the real part of the relative permittivity of the dielectric material, as in [P1]. In all three cases, the parallel component (E_z) near the center of the dipole is not much affected by the surface, and its behavior is quite similar in free space and when there is a dielectric surface.

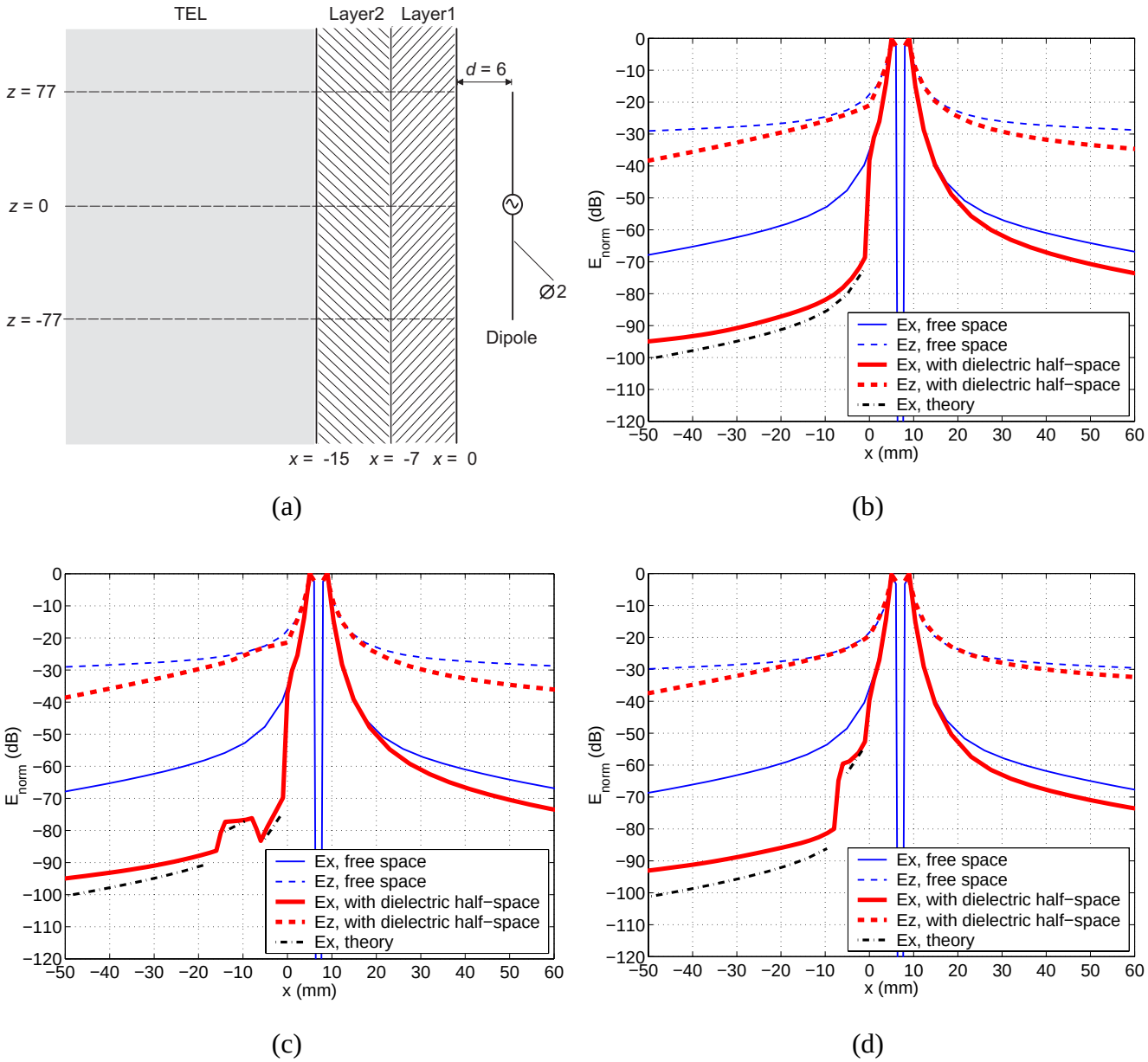

Figure 3.1 *a) Geometry of the simulation model, y = 0 mm. The dimensions and coordinates are in millimeters. b) - d) Normalized electric field components in free space and when dielectric material fills the half-space x ≤0 mm, y = 0 mm, z ≈0 mm. Dielectric half-space consists of b) TEL c) TEL+ bone (Layer2) + muscle (Layer1) d) TEL + fat (Layer1).*

To further illustrate the behavior of different field components of a dipole, Figure 3.2 shows the normalized E_x, E_z, and E_{tot} (total field) in free space and at the surface of dielectric half-space as a function of z [P1]. In the figures, $y = 0$ mm (the plane containing the dipole feed point), and $x \approx -1$ mm. As the dielectric half-space is located at $x \leq 0$ mm, the plotted values are taken just below the dielectric surface. In free space, the values are recorded at the same distance from the dipole ($d \approx 7$ mm).

In high-permittivity tissues, like tissue-equivalent liquid and muscle, the *SAR* maximums are located near the dipole feed point, as the *SAR* value is directly proportional to the total E-field in the tissue. The *SAR* maximum in these kinds of cases can be found in a location with low total original electric field but significant components parallel to the surface of the tissue (see Figures 3.2a and b). On the other hand, for low-permittivity tissues, like fat, the *SAR* maximums are found near the dipole ends, and thus close to the locations of the electric field maximums without the tissue, because the

attenuation of the perpendicular components is only moderate (see Figure 3.2c). Therefore, the results of [P1] also give a physical reason for the different peak *SAR* locations with muscle or fat layer reported in [52]. These results also suggest that from the *SAR* point of view, small loop antennas should be advantageous owing to their low E-fields.

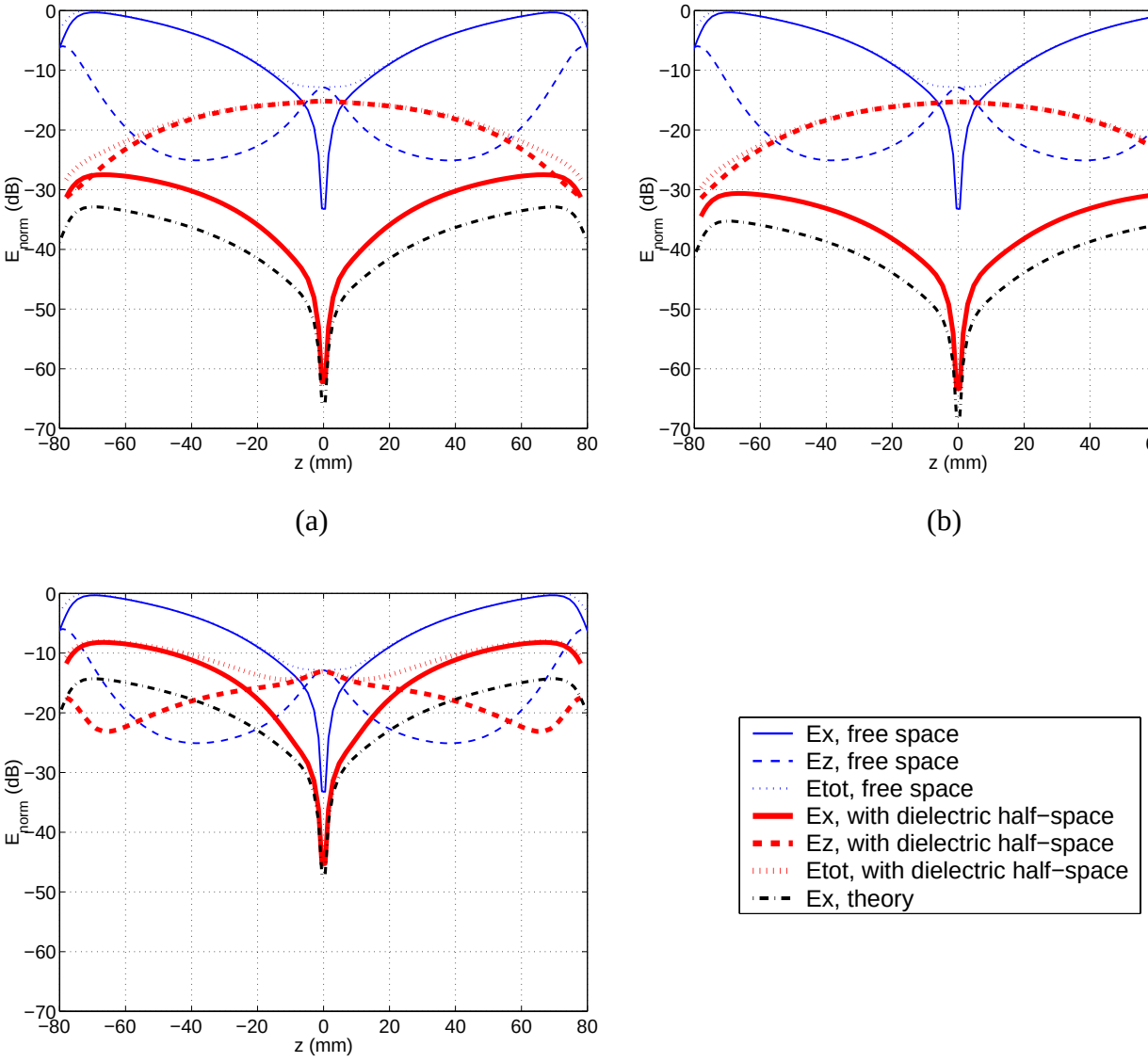

Figure 3.2 *Normalized electric field components in free space and at the surface of dielectric half-space, y = 0 mm, x ≈ - 1 mm. Dielectric half-space consists of a) TEL b) TEL+ bone (Layer2) + muscle (Layer1) c) TEL + fat (Layer1) [P1].*

The study of [P1] was extended to a more realistic case by replacing the dipole with a 900-MHz patch antenna on a handset chassis. The chassis length was 120 mm, representing roughly a typical modern mobile phone chassis. The simulation results of this patch-chassis combination showed similar *SAR* characteristics than with the dipole. This could be expected, as the radiation properties of this kind of structure resemble those of a half-wave dipole (see Chapter 4). Later, the results of the patch-chassis combination were confirmed by measurements, as the investigations of [P1] were based entirely on simulations. The *SAR* distributions in a flat phantom filled with fat-simulating liquid were measured using DASY4 equipment by Schmid and Partner Engineering AG. Rapeseed oil was used for modeling the fat tissue. The measured values for the liquid parameters were $\varepsilon_r' \approx 3$ ($\varepsilon_r' = 5$ in the simulations),

$\sigma_{\text{eff}} \approx 0.01$ S/m ($\sigma_{\text{eff}} = 0.025$ S/m), and $\rho \approx 900$ kg/m^3 ($\rho = 1100$ kg/m^3). The measured *SAR* maximums in the fat-simulating liquid were located near the chassis ends. Thus, the so far unpublished measurement results fully support the simulated ones and the conclusions drawn in [P1] on the main absorption mechanism.

4 Combination of antenna and chassis

The printed circuit boards (PCB) of current mobile terminals generally have a well-grounded layer. In addition, metal shields at least on one side of the PCB are commonly used for EMC (electromagnetic compatibility) purposes. The grounding layer of the PCB and the radiation shield typically form a metal chassis for a mobile terminal. The dimensions of the chassis may vary a lot depending on the handset design. In current monoblock mobile terminals, the typical length is in the range of 80-140 mm, the width in the range of 40-60 mm, and the thickness a few millimeters. In clamshell-type terminals or phones with a slider, the chassis dimensions change in different use positions.

The chassis is an important but often less considered factor of handset antenna design. However, it has been known for years that the electrical characteristics of a mobile handset antenna depend strongly on the size of the metal parts of the device on which the antenna is mounted and the position of the antenna on it [55], [56]. The antenna couples currents on the metallic parts, and the device itself works as part of the antenna. Thus, an appropriate selection of the chassis parameters is required for an optimum antenna performance, as the bandwidth, efficiency, and *SAR* characteristics of mobile phone antennas are strongly affected by the chassis. In consequence, the conventional antenna element -based approach is not adequate for an objective evaluation of the performance of mobile phone antennas, but the effect of the mobile chassis should always be included in all considerations of bandwidth, efficiency, or *SAR* characteristics.

In this chapter, the combined behavior of antenna element and phone chassis is characterized and analyzed. The focus is on the areas related to the user interaction (*SAR* and efficiency in talk position). As a basis for all further analysis in this chapter, a novel approach for understanding the combined performance of the antenna and terminal chassis is introduced [P2]. Utilizing this knowledge, the effects of different chassis parameters on antenna performance are explained. This chapter is based mainly on the results of [P2] and [P3], but also other relevant studies available in the open literature are considered. So far, all the related investigations have been conducted with monoblock terminals, but the results can also be applied to antennas of other terminal types.

4.1 Resonator-based analysis

The effect of the chassis on antenna performance has been identified in several publications. In [P2], a new approach for analyzing the problem was taken, and a simple circuit model of coupled series and parallel resonators was introduced for the antenna-chassis combination operating at one frequency range. The basic idea behind this model is that an antenna-chassis combination supports two significant, fairly independent wavemodes: the compact quasi-TEM wavemode of a self-resonant antenna element and the single-wire waveguide -type wavemode of a chassis resembling a thick dipole. The properties of the wavemodes (resonant frequency, Q-factor, field distribution) can be manipulated quite independently and their relative amplitudes can be chosen by controlling the coupling between them. These wavemodes can be used to describe both the impedance and the radiation characteristics of the antenna-chassis structure. Later, in [57] and [58], the characteristic mode theory defined in [59] has been applied to the wavemodes considered in [P2] to further analyze the behavior of the antenna-chassis structure.

The presented circuit model clarifies the interaction between a small antenna element and a finite metal plate. Based on the model, the reasons for the performances of different antenna-chassis combinations can be analyzed easily. The obtained theoretical results, which are also supported by the results of 3D simulations with phone models as well as those of prototype measurements, indicate that at 900 MHz, the contribution of the handset antenna element to the radiated power is small, typically below 10 %

[P2]. Thus, the phone chassis is actually considered the main radiator, while the antenna element works merely as a feed structure. At 1800 MHz, the effect of the handset antenna element is much more significant; a typical antenna element radiates approximately 50 % of the total radiated power. Furthermore, it is shown in [P2] that the *SAR* or efficiency beside user at 900 MHz is not improved by a patch antenna element, when compared to those obtained for the chassis without any antenna. Therefore, as most of the radiation is produced by the currents of the chassis, they are also the most significant aspect from the *SAR* point of view. At 1800 MHz, the contribution of the chassis currents on *SAR* and efficiency beside user was found to be smaller but still significant.

4.2 Effect of chassis on the bandwidth

According to the fundamental limit for the radiation quality factor (see Section 2.1.1), such bandwidths as required for mobile terminals cannot be obtained with antennas whose size is that of the handset antenna element. Apparently, a larger current distribution is needed, and that is provided by the chassis wavemode. Therefore, the total bandwidth of an antenna-chassis combination depends both on the bandwidth of the antenna element and on the coupling to the chassis resonance [P2]. The chassis wavemode explains the extremely large bandwidths presented in some publications, e.g. in [60] a 32 % impedance bandwidth ($L_{retn} \geq 10$ dB) at the center frequency of 2.03 GHz was reported for a $12.5 \times 27.0 \times 3.5$ mm^3 (length × width × height) meandered dual-element located on an FR4 substrate of 72×30 mm^2.

Chassis length

Research on the effect of chassis on the bandwidth performance has mainly focused on the chassis length [P2], [P3], [O1], [O3], [O8], [O10], [55], [56], [61], [62], [63]. In these articles, it has been shown that the bandwidth changes rapidly as a function of chassis length. This is because of the dipole -type radiation of the chassis currents [P2], [P3]. If the chassis resonates at the operating frequency of the antenna element, the amplitude of the chassis wavemode is high, and the bandwidth of the antenna-chassis combination increases strongly. When the chassis is resonant, its effective length is approximately $0.5\lambda_0$, which corresponds to the physical chassis length of $\approx 0.4\lambda_0$ [P2], [P3]. When the chassis resonance is farther from the operating frequency, the bandwidth decreases due to the smaller contribution of the chassis. See Figure 4.1 (chassis width 41 mm, chassis thickness 3.6 mm). All the referred studies are performed in free space, but in [P3] similar characteristics are also reported when a handset is located beside a user.

In general, the contributions of the antenna element and phone chassis to the radiation bandwidth depend on the design and operating frequency of the structure. The contribution of the chassis wavemode is emphasized at lower frequencies due to the smaller volume of the antenna element measured in wavelengths. Typically, the bandwidth of a planar antenna element located on a large metal plate, which does not support propagating waves, is close to the minimum bandwidth obtained for a similar antenna element on a handset chassis. This minimum is normally obtained with the most unfavorable (“antiresonant”) size of the chassis. At 900 MHz, where the chassis wavemode is clearly dominant, the maximum bandwidth obtained for a typical antenna element on a resonant chassis may be over 20 times the minimum [P2], [P3]. At 1800 MHz, the maximum is 4-5 times the minimum [P2], [P3].

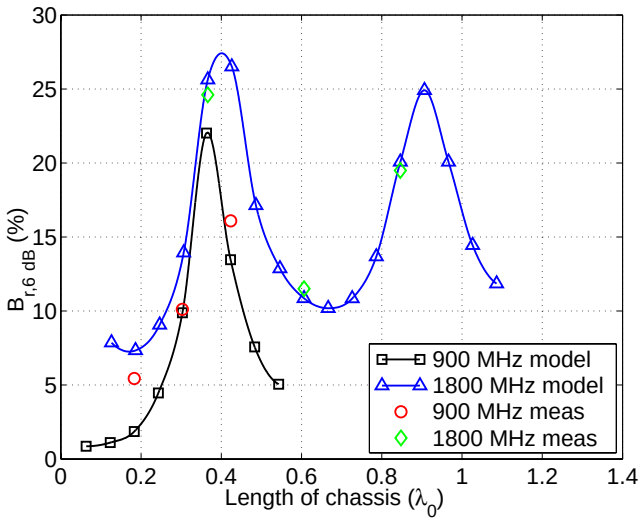

Figure 4.1 *Simulated and measured impedance bandwidths ($L_{retn} \geq 6$ dB) of 900- and 1800-MHz patch antennas in free space as a function of chassis length [P3].*

Thus, from the maximum bandwidth point of view, the ideal case is when the resonant frequency of the chassis is close to that of the antenna element. In current handset designs (chassis length of the order of 100 mm), the first order resonance of the chassis is typically around 1.1 GHz and the second order resonance is around 2.5 GHz [P2]. Therefore, for the optimal bandwidth in current cellular communications systems, the chassis resonant frequency has to be down-tuned. In a fixed-size metal plate, it can be realized by lengthening the current path by using a slotted ground plane [P2]. The same idea has been later applied at least in [64], [65]. In addition, the bandwidth can be increased by a stronger coupling to the chassis, which has been demonstrated in [P2] by extending the patch over the end of the metal plate and bending it. Also, the antenna orientation has been shown to clearly affect the obtained impedance bandwidth [P2], [P3], [66], because the orientation affects the strength of the coupling. Theoretically, by optimizing the coupling one can obtain approximately 95-100 % bandwidth ($L_{retn} \geq 6$ dB) when the resonant frequencies of the antenna element and the chassis are matched [P2].

In [P2] and [O14], it was suggested that very wide bandwidths (up to 95 %, $L_{retn} \geq 6$ dB) are possible with optimal coupling also by using practically non-radiating, non-resonant coupling elements. This issue has been further considered in [O12] and [67]. The results of [P2], [O12], [O14], and [67] show that a standard coupling element (antenna) can be used in several designs and only the matching circuit for it has to be redesigned. The results also demonstrate that simple, very compact antenna structures are possible to realize. A prototype studied in [O12] and [67] has a volume of only 1.3 cm^3, which is about one fourth of the size of a typical dual-band PIFA (planar inverted-F antenna) of a mobile phone, and still the performance is competitive to the traditional PIFAs. In this study, the purpose was to excite the chassis currents as efficiently as possible while minimizing the size of the coupling element. However, as was discussed in Chapter 2, the size is always closely connected to the bandwidth and efficiency. Therefore, these three parameters could be emphasized differently.

Chassis width

The effect of the chassis width on bandwidth was studied in [P3], [63]. Generally, the results follow the behavior of chassis length [P2], [P3]. In [P3], it is shown that the bandwidth of the antenna-chassis combination increases when the chassis approaches the resonant width. Wide bandwidths are also obtained when the chassis is narrower than the antenna element owing to the strong coupling to the chassis wavemode.

Chassis thickness

In addition, the effect of the chassis thickness on bandwidth was studied for 1.1 - 11.1 mm-thick chassis at 900 and 1800 MHz in [P3]. The chassis length and width were 101 and 41 mm, respectively. With the studied structures, the chassis thickness was noticed to have only a minor effect on the impedance bandwidth - the changes as a function of chassis thickness were one percent unit at the maximum. At 900 MHz, the bandwidth ($L_{retn} \geq 6$ dB) was approximately 10 % for each chassis thickness. At 1800 MHz, the corresponding value was 11 %.

4.3 Effect of chassis on the SAR characteristics and efficiency in talk position

Besides the bandwidth, another important design consideration of handset antenna-chassis combination involves the interaction of electromagnetic radiation with human body. This is a topic, which has been given less consideration until quite recent studies.

Chassis length and width

In [63], the effects of the chassis length and width on the performance of a helical and a patch antenna were investigated by FDTD (finite-difference time-domain) simulations at 900 MHz. A spherical homogenous head model surrounded with a shell representing the skull was used. The minimum distance between the phantom and the chassis was 8 mm. As a general remark about this study, it could be said, that the head model is considered unrealistic because of a low-effective-conductivity skull instead of a high-effective-conductivity skin as the outermost layer. Thus, the material parameters used in the skull (relatively low ε_r' and σ_{eff}, high ρ) probably caused very low *SAR*s near the surface of the head. However, no absolute *SAR* values or the locations of the *SAR* maximums were given in the paper. In addition, owing to the spherical shape of the head model, only very small part of the phone chassis can be located at the minimum distance from the head. It was reported that as the chassis approaches the resonant length, the extended current distribution increases the bandwidth, and the attenuated maximum current causes a reduction in the 10 g average *SAR*s. On the other hand, considering the novel information relating to the general energy-absorption mechanism [P1], the attenuated maximum current does not explain the decreased *SAR*s with the chassis of resonant length. The efficiency characteristics were not reported in this paper.

In [68], the effect of different chassis lengths on *SAR*s generated by mobile phones with integrated antennas was studied with FDTD simulations. Phone models with antennas at 900 MHz and 1800 MHz were studied with a distance of 5 mm to the surface of a flat phantom filled with homogeneous tissue-simulating liquid. Generally, two maximums were found in the *SAR* distribution at 900 MHz, one near the shorting edge of the antenna element and the other - higher - near the vertical center of the chassis. At 1800 MHz, the coupling of the antenna element to the chassis is smaller, and the highest *SAR* maximum appeared near the shorting edge of the antenna. In this study as well, the lowest *SAR* at 900 MHz was reached when the chassis was close to the resonant length. In addition, a direct relation was observed between the distribution of the surface current density on the PCB and the distribution of *SAR*. This finding has its basis on the old common belief on the general energy-absorption mechanism [51]. However, if this study was made with low-permittivity tissue as the outermost layer, based on [P1], it could be assumed that there would not be a direct relation between the current density and *SAR*. The efficiency was not considered in this paper either.

Despite these two studies, so far a systematic characterization and analysis of the chassis effect on antenna performance was not carried out. As a part of this thesis, in [P3], a comprehensive study of this issue was performed, including also an investigation of the radiation efficiency with different chassis parameters. The paper presents a study of two coarse phone models, which comprise an internal patch antenna and phone chassis, and are positioned in actual handset use position beside an anatomical, heterogeneous head model. One of the phones is for 900 MHz and the other for

1800 MHz. The approach is based on the modal analysis [P2]. The main part of the study is based on FDTD simulations, but some measurement results are also presented to validate the simulations. Parts of this study were also published in [O8], [O10], and [69].

Contrary to the previous publications on the effect of chassis length to *SAR* [63], [68], this paper [P3] shows that at chassis resonances with bandwidth maximums, also the *SAR* caused by the phone reaches its maximum values. *SAR* trends similar to those in [P3] can also be noticed in [70], in which the *SAR* behavior of different size patch antennas located on chassis of constant sizes, which were positioned beside an anatomical head model, were investigated as a function of frequency. Thus, the type of the used phantom is significant when considering the *SAR* characteristics. The results seem not to be very sensitive to the differences in the anatomical head model type [P3], but the shape of the phantom is significant (anatomical, spherical, or flat phantom). The different phantom shapes cause the internal electric fields, and thus the *SAR* characteristics, to be dissimilar. However, the results for both anatomical phantom and flat phantom are important: the anatomical phantom describes the situation in the traditional talk-position while the flat phantom provides trends for body-worn terminals. At the same time with *SAR* maximum in the anatomical head, a decrease in radiation efficiency occurs compared to the general trend [P3]. This is illustrated in Figure 4.2. The same phenomenon can be observed in the results of [70]. With a flat phantom as well, there are minimums in the radiation efficiency at bandwidth maximums [P3], even though the *SAR* does not follow the same trend.

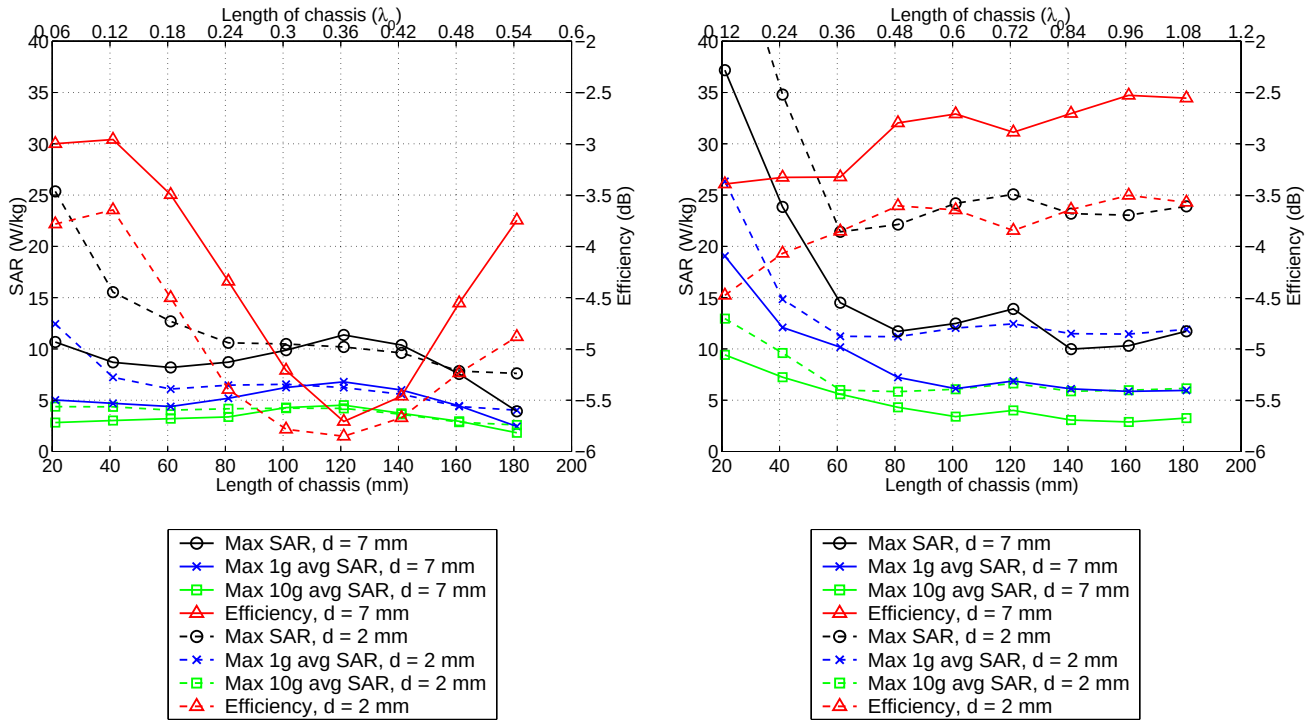

(a) (b)

Figure 4.2 SAR*s and radiation efficiencies as a function of chassis length at a) 900 MHz and b) 1800 MHz. Solid lines represent cases where distance from head to phone d ≈ 7 mm. Dashed lines represent cases where d ≈ 2 mm.* P_{in} *= 1 W [P3].*

According to [P2] and [P3], at 900 MHz, the antenna element does not contribute much to the *SAR*, which is mainly caused by the dipole -type resonant mode of the chassis. The *SAR* maximums are generally located near the vertical center of the chassis, excluding the shortest chassis lengths (Figure 4.3a). At 1800 MHz as well, the *SAR* maximums are located near the vertical center of the chassis when the chassis length is close to the first resonant length (Figure 4.3b). For longer chassis, two local *SAR* maximums can be observed. The first maximum is located under the antenna element, and the

second one lower in the chassis area, indicating that the chassis wavemode has a considerable contribution to the *SAR*s also in these cases. These results suggest that at 1800 MHz frequency range it is possible to some extent optimize both bandwidth and *SAR* (or efficiency) by designing the antenna element so, that local *SAR* maximums are avoided. At 900 MHz, the chassis is the main source of radiation, and therefore, the only possibility to affect the *SAR* obtained with a certain size of chassis is to control the chassis currents. This issue has been studied later in [71], in which a technique to increase the efficiency of a handset placed beside a user was proposed for a 900/1800 MHz dualband phone with a PIFA antenna. The improvement was designed for 900 MHz, because the contribution of the chassis wavemode is dominant. The method was to add a parasitic radiator into the structure on the opposite side of the chassis where the antenna is located. It was realized as a metallic casing around the phone display. *SAR* is reduced owing to the currents on the parasitic radiator, which are of opposite phase to the currents of the chassis, and therefore cause a cancellation of the near field on the user's side of the chassis. It was demonstrated that at 900 MHz, the *SAR* is reduced by 6 dB, and the efficiency is improved by 1.2 dB when the handset is located beside the user's head. The *SAR* and efficiency at 1800 MHz remained unchanged. As drawbacks, the free space efficiency at 900 MHz is reduced by up to 4 dB, and the bandwidth is decreased significantly. A similar method for optimized *SAR* was proposed in [72].

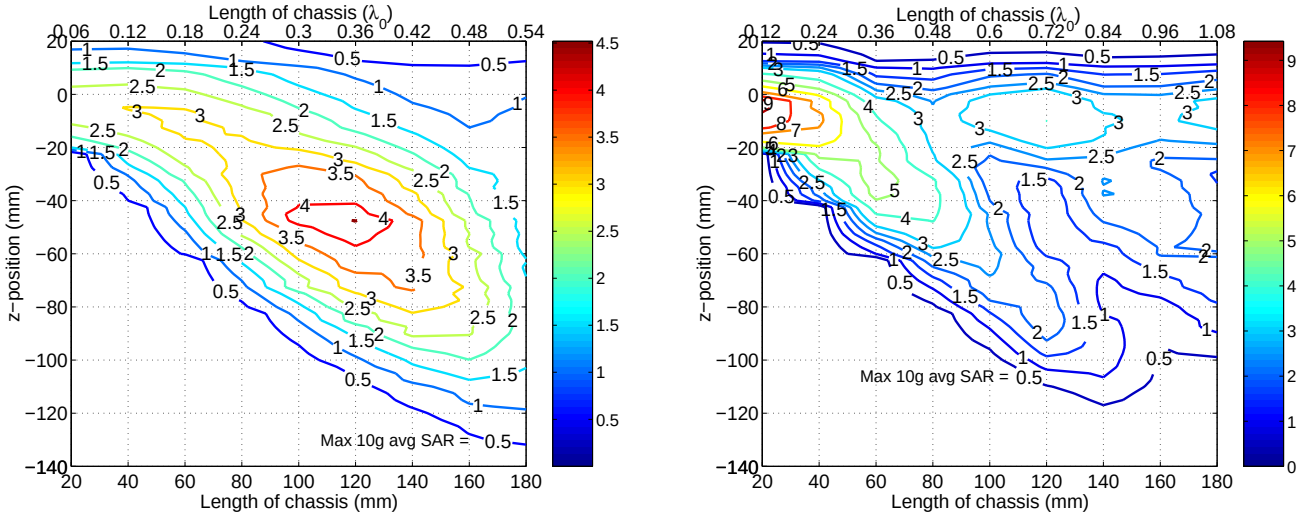

(a) (b)

Figure 4.3 *Distribution profiles of maximum 10 g average SARs (W/kg) in head at a) 900 MHz (Max. ≈4.5 W/kg) and b) 1800 MHz (Max. ≈9.4 W/kg). Distance from head to phone d ≈7 mm. Color figure can be viewed in [P3].*

The effect of the chassis width on antenna performance was studied with two different chassis lengths, l_c = 61 mm and l_c = 101 mm [P3]. At 900 MHz, the shorter chassis is clearly non-resonant, and the resonant frequency of the larger chassis approaches the resonant frequency of the antenna element. At 1800 MHz, the situation is the opposite. At both frequencies, when the chassis is narrower than the antenna element (41 mm), and the bandwidth is increased due to the strong coupling to the chassis wavemode, the *SAR*s increase and the radiation efficiencies decrease strongly (Figure 4.4). Then the *SAR* maximums are located near the vertical center of the chassis with the chassis near the resonant lengths, and their values are higher than those with the non-resonant chassis lengths. The bandwidth also increases owing to the larger contribution of the chassis wavemode when the chassis width approaches resonance. At this point as well, an increase in the *SAR*s can be observed.

Based on these results [P3], it can be claimed, that when a phone with a patch antenna is positioned in actual handset use position beside an anatomical head, there is a connection between the impedance bandwidths, *SAR*s, and radiation efficiencies: higher *SAR* values and lower radiation efficiency are

obtained in cases where the bandwidth increases due to the strong excitation of the chassis wavemode. In these cases, the reduced peak *SAR* can be seen as an increase in the antenna efficiency. The results are considered to represent the typical characteristics of internal mobile phone antennas and can be generalized to apply to any similar patch -type antenna elements. The presented characteristics can be applied to dualband or multiband antenna elements as well, and scaled to other frequency ranges, even though the study of [P3] is realized for 900 MHz and 1800 MHz antenna elements separately.

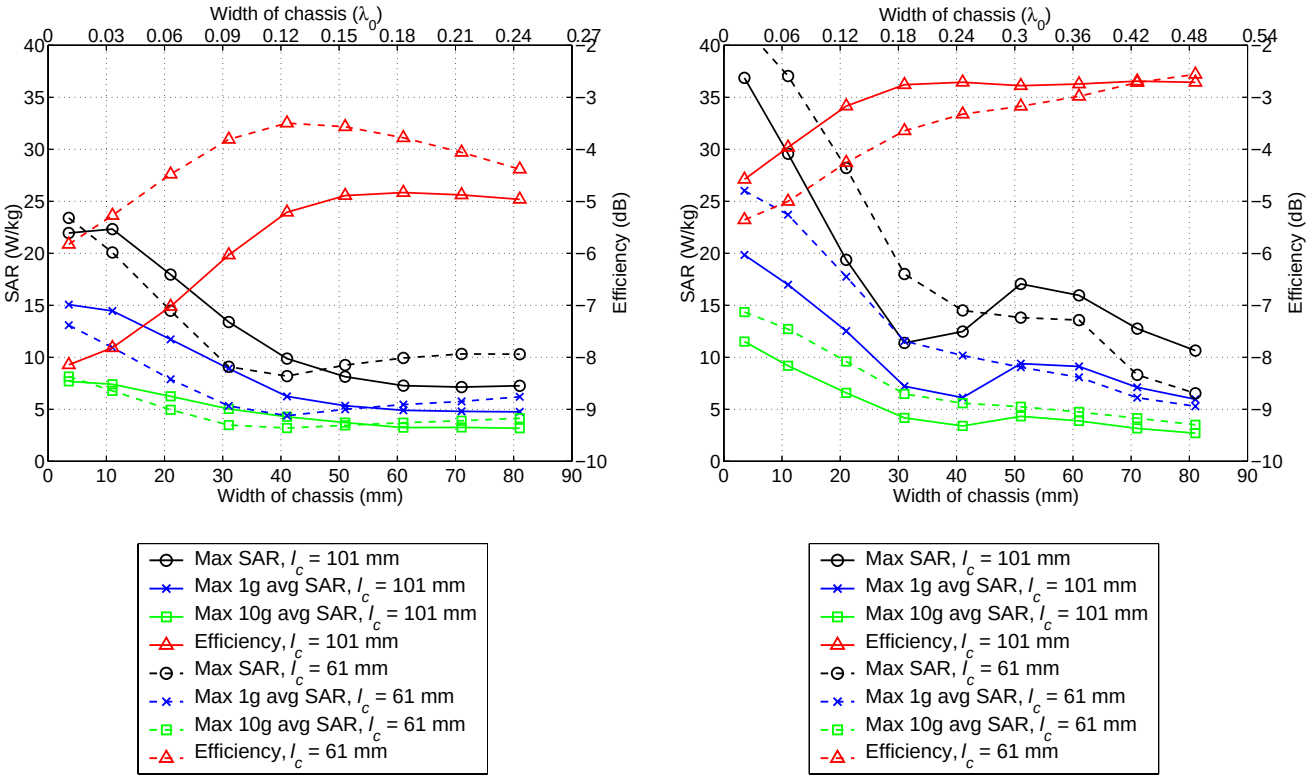

(a) (b)

Figure 4.4 *SARs and radiation efficiencies as a function of chassis width with two chassis lengths (l_c = 101 mm and l_c = 61 mm) at a) 900 MHz and b) 1800 MHz. Distance from head to phone d ≈ 7 mm. P_{in} = 1 W [P3].*

Distance of the chassis from the head and chassis thickness

In the literature, several studies concerning *SAR* or radiation efficiency as a function of distance between the head and phone model can be found, e.g. [11], [12], [39], [73], [74]. According to these studies, the closer the phone is to the head, the less the antenna input power is radiated into the free space, and the higher the *SAR* values and the lower the radiation efficiency are. In most of the published studies, the phone is located relatively far from the head surface even with the nearest studied positions, as the distance is typically varied roughly from 10 to 60 mm. In addition, the thickness of the phone chassis (usually over 20 mm) increases further the distance between the antenna element and the head. When modern handsets are considered, the typical distance between the phone chassis (metal thickness ≈ 2-5 mm) and the user's head is approximately 3-12 mm assuming a handset covered with plastic casing. Studies, where the phone is within this distance are reported e.g. in [O2], [61], [63], [68]. However, no results regarding the effect of distance between the phone and head were given in these papers. This subject was studied in [P3]. As could be assumed based on the previous studies, the *SAR*s decrease and the radiation efficiencies increase as the distance from the head to chassis increases. However, the results give novel information, as it was noted that when the chassis is close to resonant, the *SAR*s decrease slower as a function of distance than when the chassis is non-resonant.

The effect of the chassis thickness (1.1 - 11.1 mm) was studied in [P3] as well (chassis length and width 101 and 41 mm, respectively). No other study of this issue could be found in the literature. The distance between the head and chassis was kept constant in all cases ($d \approx 7$ mm), thus also the distance between the head and antenna element increased as a function of chassis thickness. The general trends in the *SAR*s and radiation efficiency are those as could be expected: due to the weaker near fields the *SAR*s in the head decrease and the radiation efficiencies increase as the chassis thickness is increased. Therefore, it is important to use a realistic chassis thickness, which is typically a few millimeters in current mobile terminals, as the *SAR* and efficiency results for thicker chassis often used in the literature (roughly 20 mm) are quite different from those for typical modern handsets. Also, it was noticed that both at 900 MHz and at 1800 MHz, the *SAR*s and radiation efficiencies at equal distances between the head and antenna element, and thus equal distances between the head and antenna side of the chassis, are roughly equal regardless of the chassis thickness.

Hand

As a hand is always present in a typical operating situation of a mobile phone, the effect of the user's hand with different chassis parameters was investigated in [P3]. The whole study was performed in the presence of the anatomical head model. Two different block models of the hand were tested. Both models consisted of two tissues, bone surrounded by muscle. The first one was similar to a typical hand model used in the literature [12], [13] and modeled mainly the palm, while the fingers were very short. The second model, developed in this work, simulated a more realistic way in which a small handset is held. The fingers of this model were clearly longer, and the thumb held one edge of the chassis and the rest fingers the other.

Similar general behavior in the *SAR*s in the head was observed with either one of the hand models than when the hand was not present [P3]. The trends in the radiation efficiencies were also similar to those obtained without hand. As expected [13], the worst-case *SAR* values in the head were obtained without hand, because the hand absorbed part of the power. The *SAR* values in the hand models used in this work were clearly lower than the specified maximum value (see Table 2.1). However, concerning the efficiency of the antenna-chassis combination, it is necessary to consider also the effect of the hand, as the decrease in efficiency due to the hand may be several decibels. In [P3], the reported efficiency reductions due to the hand were between 2 and 6 dB at 900 MHz, and between 1 and 7 dB at 1800 MHz, depending on the chassis parameters, hand model and also on hand location. The largest reductions in radiation efficiencies occurred when the hand covered those parts of the phone that are the main contributors to the radiated power.

5 Dielectric resonator antennas

Traditionally dielectric resonators (DR) have been used mainly for energy storing in microwave circuits such as oscillators, in which the resonators are enclosed by metal shields [75]. The electromagnetic fields of a DR extend over the geometrical boundary of the resonator. Hence, open DRs are useful as radiators if the feed mechanism, geometry, excited wavemode, and material of the resonator are chosen appropriately. Since the first reported use of a DR as an antenna element [76], numerous studies of dielectric resonator antennas have been published. Antenna elements with different shapes such as rectangular, cylindrical, and hemispherical; with different materials ($\varepsilon_r' \approx 10$-100); and with different feeding methods including probes, slots, microstrip lines, coplanar waveguides, and conformal conducting strips have been studied extensively. A good review is presented in [77].

The main purpose of the work in this thesis was to study whether DRAs could be used as small internal antennas of mobile terminals. The focus was on rectangular dielectric structures. The preliminary work concentrated on characterizing the basic properties of DRAs (Section 5.1). The main emphasis was put on the behavior of radiation efficiency of antennas miniaturized using high-permittivity materials, as this subject had been given less attention previously. As promising results were obtained, the work on the use of DRAs in mobile terminals was continued, and a novel wideband DRA for mobile phones was developed (Section 5.2). Other recently published studies of DRAs in mobile terminals are also reviewed in this section.

5.1 General characteristics of DRAs

The dimensions of a dielectric resonator antenna are approximately proportional to $(\varepsilon_r')^{-1/2}$ because the wavelength in the material (λ_r) depends on the value of the relative permittivity according to $\lambda_r = \lambda_0 / (\varepsilon_r')^{1/2}$, where λ_0 is the free space wavelength. If needed, DRAs can be built very small because high permittivity (up to $\varepsilon_r' \approx 100$) low-loss ($\tan\delta \approx 2.5 \cdot 10^{-4}$ or less) materials are commercially available. However, the higher the relative permittivity is, the more the electromagnetic fields are restricted within the dielectric. Consequently, the smaller the radiating aperture will be, which leads to decreased radiation and therefore decreased efficiency. In addition, the narrower frequency band the antenna will have.

High efficiency is generally considered a major merit of DRAs. Dielectric losses of DRAs are typically very small, although the material loss factor normally increases slightly when ε_r' increases. In general, the conductor losses of DRAs are small compared to those of other typical small antennas, such as microstrip patches, because DRAs have less metal parts. The power loss in conducting portion may reduce the efficiency of typical metal antennas significantly especially at higher frequencies, as conductor losses increase with the square of the operating frequency.

As a part of this thesis, in [P4], the size reduction of rectangular half-volume (HV) DRAs was investigated experimentally by increasing the relative permittivity of the dielectric material. The emphasis was on the behavior of radiation efficiency, as this information was not available in the open literature. The geometrical shape of all the studied antennas remained unchanged, but the material permittivity was increased to shrink the antenna ($\varepsilon_r' = 2$ - 70). One edge of the dielectric element was metallized to form a half-volume structure similar to that presented in [78]. The prototypes were located on large ground planes compared to the size of the antenna to avoid the effects due to currents induced into the mobile terminal size metal plate, which were discussed in the previous chapter. The radiation efficiency of the studied antennas was observed to decrease as a function of permittivity, as

could be expected. Still, the radiation efficiency of the prototypes stayed fairly high also for high values of ε_r', e.g. $\eta_r \approx 86$ % for ε_r' = 70, which gives a good basis for the miniaturization of HV-DRAs.

The efficiency of miniaturized antennas was further investigated by studying theoretically the metal losses of DRAs and dielectrically loaded patch antennas. Four basic antenna elements were selected for the study: DRA, HV-DRA, half-wave patch, and quarter-wave patch (see Figure 5.1). The design criterion was to keep the resonant frequency approximately equal for all the studied antennas, while the sizes of the antennas were scaled using materials with different permittivity. The antennas were located on large ground planes.

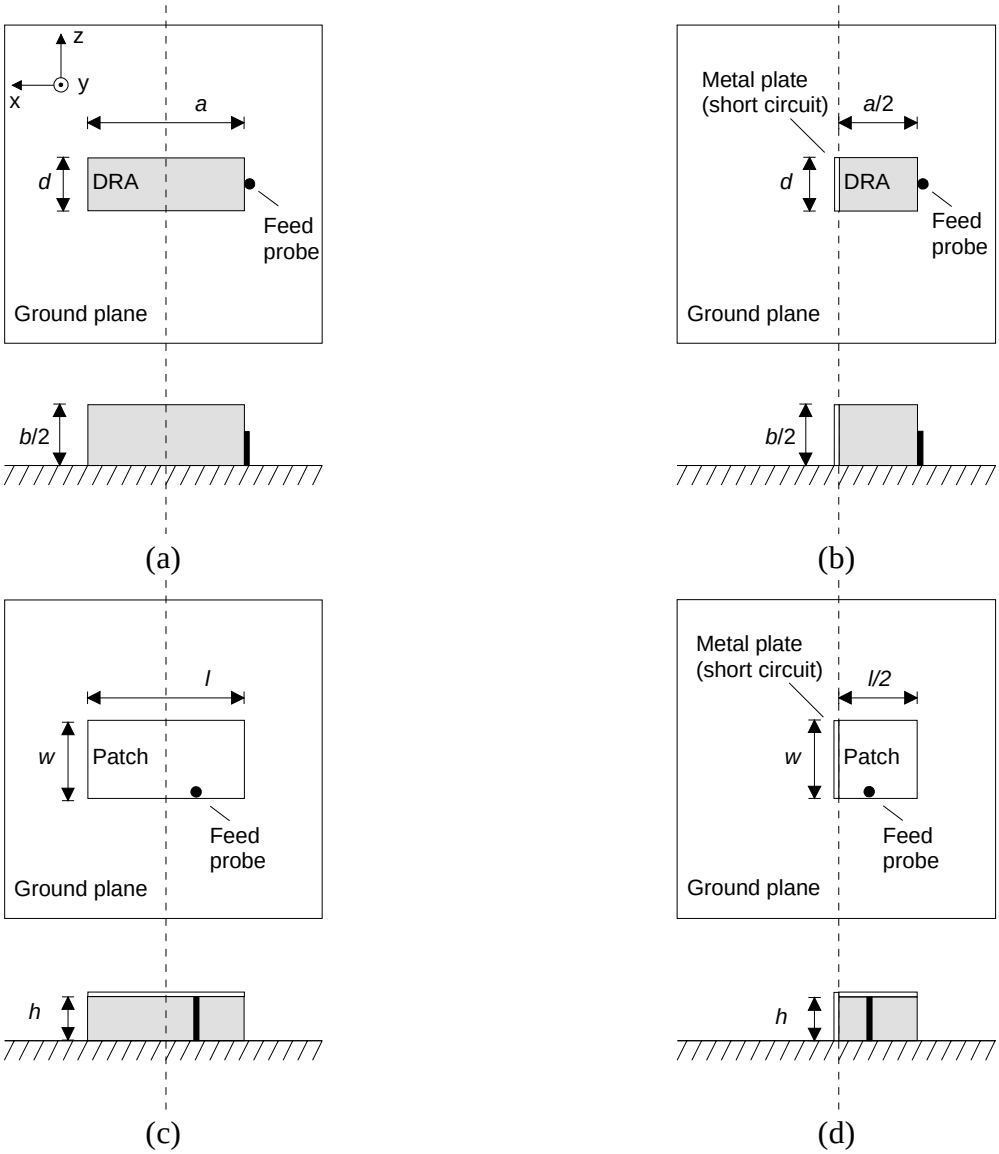

Figure 5.1 *Structures of the studied antennas. a) Dielectric resonator antenna, b) Half-volume dielectric resonator antenna, c) Half-wave patch, d) Quarter-wave patch.*

The DRAs were rectangular structures excited by the lowest order wavemode ($TE_{11\delta}$). The ratios of the dimensions were similar to those in [P4]. All the antenna dimensions were scaled according to the relative permittivity, thus the antenna shape was preserved. Nevertheless, in HV-DRAs, some small modifications to antenna dimensions were needed to reach the design goal of approximately constant resonant frequency. With the DRAs ε_r' = 12…200, and with the HV-DRAs ε_r' = 12…150. The lengths and widths of the patches were scaled according to ε_r', but the antenna heights were kept constant. Two different antenna heights were selected: 2 and 4 mm. In the half-wave patches, the antenna

lengths were approximately twice the widths. In the quarter-wave patches, the lengths and widths were approximately equal. With the half-wave patches $\varepsilon_r' = 1\ldots70$, and with the quarter-wave patches $\varepsilon_r' = 1\ldots38$.

The approximate equation for the quality factor due to metal losses (Q_c) for a patch and the associated ground plane has been derived e.g. in [79]. The surface current density is first found from the magnetic field assuming perfect conductivity; the power loss is then given by the surface integral of the surface resistance times the square of the surface current density. The total stored energy is given by twice the volume integral of the square of the magnetic field, as the stored electric energy equals the magnetic energy at resonance. The metal losses for the short circuit in a quarter-wave patch and the metal parts of DRA (ground plane) and half-wave DRA (ground plane and short circuit) were derived following the same approach. The magnetic field components of DRAs were obtained from [80]. In addition, the DRA wavenumbers satisfy the following equations: $k_x^2 + k_y^2 + k_z^2 = \varepsilon_r' k_0^2$, $k_x = \pi / a$, $k_y = \pi / b$, $k_z \tan(k_z d/2) = \sqrt{(\varepsilon_r' - 1)k_0^2 - k_z^2}$ [80]. The resulting approximate equations for the Q_cs are given in Table 5.1.

Table 5.1 *Approximate equations for the quality factors due to metal losses.*

λ/2-patch / λ/4-patch + ground plane	$Q_{c1} = h\sqrt{\mu_0 \pi f_r \sigma}$
Short circuit of the λ/4-patch*	$Q_{c2} = l\sqrt{\mu_0 \pi f_r \sigma}$
λ/4-patch + ground plane + short circuit	$Q_{c3} = \left(\frac{1}{Q_{c1}} + \frac{1}{Q_{c2}}\right)^{-1}$
Ground plane of the DRA / HV-DRA	$Q_{c4} = \frac{b}{2}\sqrt{\mu_0 \pi f_r \sigma}\,\frac{\left[\left((k_x k_z)^2 + (k_y k_z)^2\right)\left(1 - \frac{\sin(k_z d)}{k_z d}\right) + (k_x^2 + k_y^2)^2\left(1 + \frac{\sin(k_z d)}{k_z d}\right)\right]}{(k_x k_z)^2\left(1 - \frac{\sin(k_z d)}{k_z d}\right) + (k_x^2 + k_y^2)^2\left(1 + \frac{\sin(k_z d)}{k_z d}\right)}$
Short circuit of the HV-DRA	$Q_{c5} = \frac{a}{2}\sqrt{\mu_0 \pi f_r \sigma}\,\frac{\left[\left((k_x k_z)^2 + (k_y k_z)^2\right)\left(1 - \frac{\sin(k_z d)}{k_z d}\right) + (k_x^2 + k_y^2)^2\left(1 + \frac{\sin(k_z d)}{k_z d}\right)\right]}{(k_y k_z)^2\left(1 - \frac{\sin(k_z d)}{k_z d}\right) + (k_x^2 + k_y^2)^2\left(1 + \frac{\sin(k_z d)}{k_z d}\right)}$
Ground plane and short circuit of the HV-DRA	$Q_{c6} = \left(\frac{1}{Q_{c4}} + \frac{1}{Q_{c5}}\right)^{-1}$

*The length of λ/4-patch is l/2.

The resonant frequencies and radiation quality factors of the antennas were determined by simulations using a commercial FDTD-based electromagnetic solver (Semcad by Schmid and Partner Engineering), as no precise methods could be found for determining those theoretically. All the metal parts as well as the dielectrics were modeled lossless, because the metal losses could not be modeled with the software, and the dielectric losses were assumed negligible compared to the conductor losses. The radiation efficiencies for the antennas were calculated according to the simulated Q_r and the theoretical Q_c. The conductivity value used in the calculations was $\sigma = 1.9 \cdot 10^6$ S/m (value for tin

bronze). The resonant frequencies of the antennas are 2500 MHz ± 5 %. The resulting values for Q_r, Q_c, and η_r are plotted in Figure 5.2.

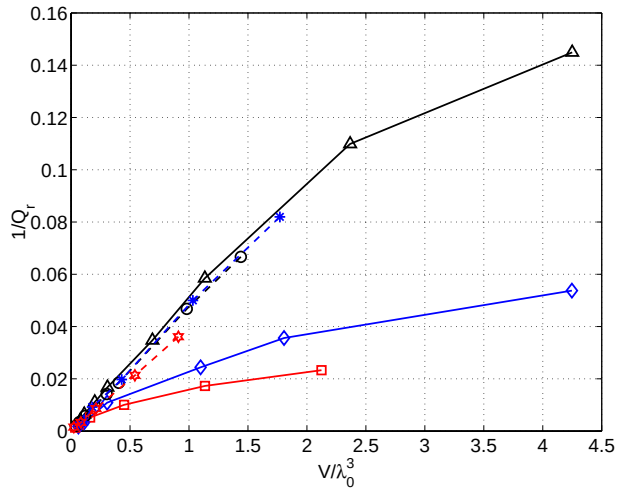

(a)

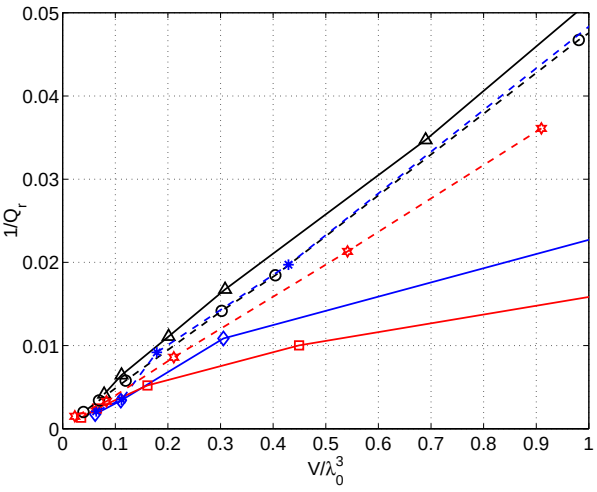

(b)

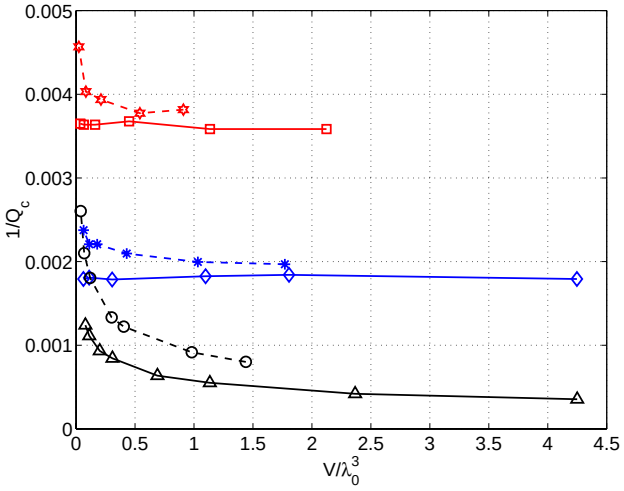

(c)

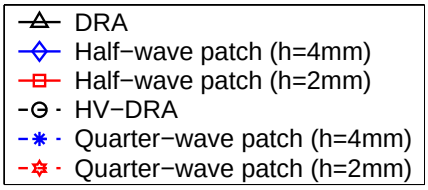

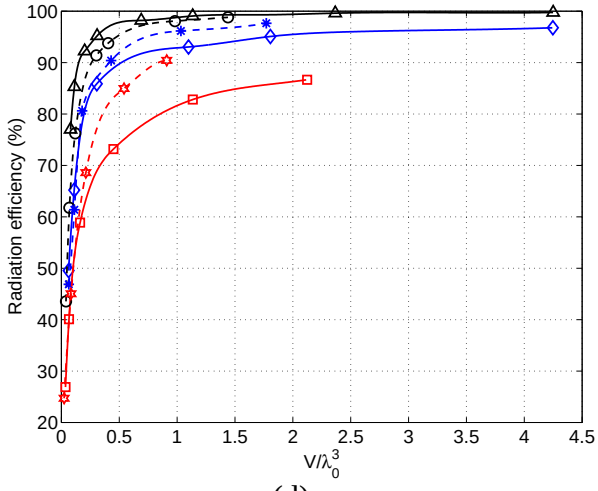

(d)

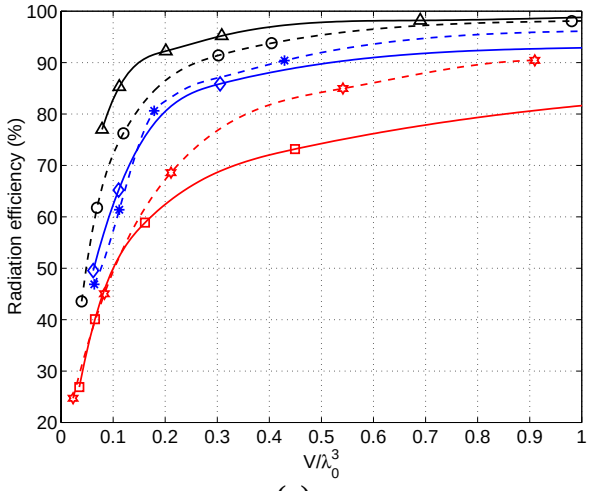

(e)

Figure 5.2 *a) Inverse of the radiation quality factor vs. antenna volume in free space wavelengths V/λ_0^3 $[(cm^3/m)\cdot 10^{-3}]$, b) Closer view of a), c) Inverse of the conductor quality factor vs. antenna volume in free space wavelengths, d) Radiation efficiency vs. antenna volume in free space wavelengths, e) Closer view of d).*

To get a clearer idea of the studied antennas in practice, details of a few structures are briefly presented as examples. The dimensions of the DRA with $V/\lambda_0^3 = 0.201$ are $14.0 \times 6.9 \times 3.2$ mm^3 and $\varepsilon_r' = 100$. For the DRA with $V/\lambda_0^3 = 1.13$, the dimensions are $25.6 \times 11.6 \times 5.8$ mm^3 and $\varepsilon_r' = 30$. The quarter-wave patch ($h = 4$ mm) with $V/\lambda_0^3 = 0.179$ is filled with material having $\varepsilon_r' = 16$, and the patch area is 9.0×8.0 mm^2. For the quarter-wave patch ($h = 4$ mm) with $V/\lambda_0^3 = 1.03$ the patch area is 21.0×21.0 mm^2 and $\varepsilon_r' = 2$.

Due to fewer metal parts, DRAs have lower conductor losses and thus higher radiation efficiencies than patches (Figure 5.2), as expected. These results confirm the earlier experimental results of [P4] that the metal losses are not very significant even for quite small-size DRAs. It is also noted that the metal losses in very low-profile patches ($h = 2$ mm) are higher than in respective thicker ones ($h = 4$ mm), as a relatively larger part of the antenna surface area is metallized leading to smaller radiating aperture and consequently a larger relative contribution of metal losses. In addition, excluding the smallest antennas, the Q_rs of lower patches are higher resulting in relatively larger contribution of metal losses. According to the used approximate equations (Table 5.1), the quality factors due to patch and ground plane losses are equal with half-wave and quarter-wave patches of the same height. Thus, it is obvious that the absolute metal losses are slightly higher with quarter-wave patches due to the added short circuit. However, excluding the very smallest antennas, the radiation efficiencies of half-wave patches are lower compared to those of quarter-wave patches. This is because the contribution of metal losses is relatively larger in half-wave patches owing to higher Q_rs. With very small antennas, the losses in the short circuit become significant, as the area of the short circuit is substantial compared to all metal parts of the antenna. The results of Figure 5.2 also demonstrate that using a short circuit to halve the antenna volume is an efficient way for miniaturizing, especially for patches the additional antenna half of half-wave structures actually degrades the total performance.

5.2 DRAs for mobile terminals

Based on the results of the previous section, dielectric resonator antennas may have potential applications in mobile terminals, especially when very small antenna elements are needed. In addition to having high efficiency, DRAs are easy to incorporate into microwave integrated circuits as they can be integrated directly on the PCB of the device. So far, most of the studies have focused on demonstrating the general possibilities and advantages of DRAs for wireless applications [22], [81], [82], [83], [84], but the practical issues, regarding e.g. the finite ground plane or suitable antenna shape, have been less considered. Some DRA designs for mobile terminals are presented in the following.

In [85], a 180-degree sector of a cylindrical DRA was proposed as an internal handset antenna for the GSM1800. The antenna was located near the top of the metal plate having dimensions 100×40 mm^2. It was positioned in a way that a 90-degree sector of the antenna was on the metal plate and another 90-degree sector in the air. The volume of the antenna element was 5 cm^3 ($V/\lambda_0^3 = 1.45$), and it was fabricated from material with $\varepsilon_r' = 12$. The bottom of the half-cylinder was metallized. The measured impedance bandwidth of the structure ranged approximately from 1680 MHz to 2300 MHz ($VSWR < 2$), which satisfies easily the GSM1800-system specifications (1710-1880 MHz). Actually, the bandwidth could be reduced e.g. by fabricating the antenna with material having higher relative permittivity. At the same time, this would reduce the antenna size, which is now too large for practical handset applications. However, the shape and location of the proposed antenna element would still be rather inconvenient considering a modern mobile handset. In addition, the effect of the chassis wavemode on bandwidth has not been mentioned in the paper. The radiation pattern measurement of the proposed structure in free space shows reduced radiation towards the user's head, but no results for the *SAR* characteristics or radiation efficiency were given.

A compact DRA for WLAN (wireless local area network) applications was introduced in [86]. It consisted of a rectangular DRA ($\varepsilon_r' = 12.6$) with partial vertical and horizontal metallizations. The volume of the antenna element was only 0.18 cm^3 ($V/\lambda_0^3 = 0.964$), and it was located on the corner of a metallic plate of an FR4 board with size 85×55 mm^2. This tiny antenna in fact approaches the structure of a chip antenna. A 12 % bandwidth ($L_{retn} \geq 10$ dB) at around 5.25 GHz was reported. However, the antenna positioning was reported to have a significant effect on the bandwidth. With this structure, a 2.4 size reduction factor was obtained compared to the volume of a conventional HV-DRA with similar electrical properties. The size reduction was explained by the curvature of the field lines due to the partial electric wall boundary effect by the metal strip. Although the efficiency was not given in the paper, it can be assumed that owing to the metallizations, the losses of the proposed structure are larger compared to a traditional DRA.

In this thesis work, a small, high-efficiency, wideband DRA to be used e.g. in a mobile terminal in UMTS-system was designed [P5], [O15]. The presented antenna is simple in structure and thus easy to manufacture. Furthermore, direct integration onto the PCB of a mobile terminal is possible. The studied prototype consisted of a metal-plated FR4 PCB having size 100 mm × 40 mm and a probe-fed rectangular HV-DRA with two metallized edges (volume ≈ 2.8 cm^3, $V/\lambda_0^3 = 1.36$, $\varepsilon_r' = 16$) placed on the top corner of the PCB. This was assumed the most favorable location from the practical point of view. The reverse side of the PCB as well as the area under the DRA were left unmetallized, although in practice it is probably not preferable to remove the ground plane partially. The measured impedance bandwidth of this structure was 28 % ($L_{retn} \geq 6$ dB) at $f_c = 2.36$ GHz. The wide bandwidth was obtained owing to a novel configuration utilizing dual-resonance. This was realized by tuning the feed probe resonance and the first volumetric resonance of the dielectric dice nearly equal. The design is analogous to the design of dual-resonant patch antennas [23]; by properly adjusting the frequencies of the resonances, the coupling between them, and the coupling of the feed line to the driven resonator (here the resonant probe), a significantly wider impedance bandwidth is obtained than with a traditional single-resonant structure without increasing the size needed for the antenna. In the prototype, the bandwidth of the dual resonance was not fully optimized with respect to the matching requirement. The optimal bandwidth would be approximately 1.2 times the measured value. Neither the dimensions of the PCB were optimized with respect to the bandwidth. However, this would be complicated owing to the shaped PCB metallization. The measured radiation efficiency was high (84-99 %) over the whole impedance band.

6 Frequency-tunable antennas

Frequency tuning is one method to improve the inherently narrow impedance bandwidth of small antennas, as was discussed in Section 2.2.3. This technique enables e.g. the use of an antenna element with a smaller size than usually needed or the use of a single antenna element in several systems without increasing its size. Electrical frequency tuning can be realized by loading the antenna with an electrically controlled reactance or a passive reactance that is coupled to the antenna with a switch. In a microstrip antenna, a tunable reactance or switch is typically connected between the patch and the ground plane [29], [31], [33], [87]. Another common approach is to connect separate parts of the antenna with a tuning component [25], [88]. To maximize the frequency shift, the tuning components in such designs are typically positioned at high RF voltage or current locations, respectively, which may result in high distortion or significant losses in the tuning component. Power loss in the tuning circuit is actually a major problem of frequency-tunable antennas. Other crucial problems are the complexity and distortion owing to the non-linearity of the switches or electrically controlled reactances in the tuning circuits. In general, the main emphasis in the previous studies has been on the achievable tuning range, whereas other items have received less attention. In this thesis, low-loss tuning circuits were investigated comprehensively aiming at the minimization of power loss in the tuning circuit with respect to the achievable tuning range [P6], [O13]. This study is presented in Section 6.1. In addition, the theory of [P6] was successfully applied in [P7], in which a novel low-loss frequency-tuning circuit for mobile handset antennas was proposed. This chapter also introduces this study and presents some other state-of-the-art designs for mobile terminals.

6.1 Design method for single-resonant frequency-tunable patch antennas

A general design method for single-resonant frequency-tunable small resonant antennas was proposed in [P6] for systematic analysis and minimization of power loss in the tuning circuit. Simple circuit models for patch antennas with a fairly narrow impedance bandwidth were used to develop formulas for the theoretical calculation of the frequency shift and the associated power loss as a function of the parameters of the tuning circuit. By investigating the ratio of frequency shift and loss, an optimal configuration for the tuning circuit could be determined. The theoretical results can be used e.g. to provide optimal starting values and design curves that facilitate the final design with an electromagnetic simulator.

To support the presented theory, the design procedure was demonstrated with two example antenna structures, for which both simulated and measured results were presented [P6]. In both cases, the tuning circuit consisted of two transmission line sections connected by a PIN diode switch. The goal was to minimize the power loss in the tuning circuit and to obtain approximately equal radiation efficiencies in both switching states. The antennas were located on large ground planes to exclude the effects caused by the currents induced into the mobile terminal size metal plate (see Chapter 4). The tuning ranges of both prototypes were selected to be approximately 5 %, and their operating frequencies were around 900 MHz. As a first example, a narrowband frequency-tunable shorted patch with a very high unloaded quality factor ($Q_{0,a} = 99$) was designed. The high $Q_{0,a}$ was selected to represent a very difficult case to tune; the theoretical ratio of frequency shift and loss is inversely proportional to $Q_{0,a}$ (Eq. (6) in [P6]). Thus, any antenna with $Q_{0,a} < 99$ can be tuned an equal amount with less power lost in the tuning circuit than with this antenna. Alternatively, an antenna with lower $Q_{0,a}$ can have a larger tuning range instead of a higher efficiency. The second prototype with $Q_{0,a} = 20$ represented roughly a mobile terminal antenna for GSM900. It was designed for switching between the transmitting and receiving bands of a GSM900 mobile station. For the narrowband prototype ($Q_{0,a} = 99$) without the tuning circuit, the measured radiation efficiency at the resonant frequency was 77 %. The fairly low value is explained by the very low-profile (3 mm, $0.009\lambda_0$) antenna element (see

Section 5.1). When the tuning circuit was added, the measured radiation efficiencies at the resonant frequencies were 55 % and 68 % with the switch open and with the switch closed, respectively. For the prototype with wider bandwidth ($Q_{0,a}$ = 20), the corresponding values were 98 % (no tuning circuit), 95 % (switch open) and 95 % (switch closed). The simulated results were close to the measured ones for both prototypes. Therefore, with the proposed method, a moderate frequency tuning of even a very narrow-band antenna can be realized with fairly small reduction of efficiency caused by the tuning circuit. The designed examples and measured results clearly support the theory.

In addition, the linearity characteristics of the prototypes were studied by measurements. The tuning circuits of both prototypes caused only negligible distortion when the switch was closed. When the switch was opened, the distortion was increased and further increased when the reverse bias voltage was decreased. In this switching state, the switch was placed in a location with a high voltage over it, which is assumed the reason for worse linearity. The prototype with wider bandwidth was found to be more linear than the narrowband prototype. Based on simulations, the signal voltage over the switch was clearly higher in the narrowband prototype.

6.2 Frequency-tunable antennas for mobile terminals

Although several innovative frequency-tunable antenna designs that are intended for use in mobile terminals have been reported recently, such as [87], [88], [89], [90], [91], many practical factors, which may restrict the use and performance of certain tuning circuits in mobile terminal antennas, have been given less attention in these publications. These limiting factors are e.g. the complexity, the losses in the tuning circuit, the available dc-bias and distortion of the switching component as well as the effect of the mobile handset -size metal plate. All these issues need to be carefully considered before a certain design can find realistic applications in multisystem terminals. A few designs, which take into account at least some of the mentioned factors, are presented in this section.

In [30], different possibilities for realizing frequency-tunable PIFAs for mobile terminals operating in GSM900 and GSM1800 systems were investigated. The studied antennas were single-band devices, and they were located on large ground planes. In the most promising designs, the tuning was realized by changing the inductivity of the antenna short circuit. This was done by placing a capacitive loading in series with the short circuit. The switching was implemented by a PIN diode. The bias current was restricted to 10 mA, which is a tolerable value for mobile terminal applications. The aim was a switching solution that tunes the resonance between the transmitting and receiving bands and fully covers those bands. Based on the measured results, the prototypes did not fully satisfy the bandwidth requirements ($L_{retn} \geq 6$ dB), although the volumes of the antenna elements were large, 9.8 and 3 cm^3 at 900 and 1800 MHz, respectively. However, positioning the prototypes on a metal plate with size equal to a typical mobile terminal is likely to increase their bandwidths. At 900 MHz range, the measured radiation efficiency at the resonant frequency without the tuning circuit was 82 % and with the tuning circuit 73 % and 70 %, when the switch was open and when it was closed, respectively. At 1800 MHz range, the corresponding values were 93 % (no tuning circuit), 80 % (switch open), and 69 % (switch closed). The distortion properties were not analyzed. As a main shortcoming, these solutions required the original antenna to resonate even at lower frequencies than the desired operation band, which makes these structures ineffective from the antenna miniaturization point of view.

In [32], practical implementation issues and limitations of small narrowband frequency-tunable mobile terminal antennas were discussed. A dual-tunable shorted patch antenna structure for the US cellular (824-894 MHz) and GSM900 (880-960 MHz) systems was demonstrated. The structure had two antenna elements, one for the reception bands and one for the transmission bands. In both antennas, a PIN diode (a 3 V battery as the supply voltage) was used for switching a loading capacitor to change from one system to another. The antennas were located on a 100×40 mm^2 test ground plane consisting of real handset parts. However, the ground plane structure was not accurately described in

the article. A 10-15 MHz bandwidth was obtained with 30-40 % efficiency measured in free space with the transmitting antenna having a volume of approximately 3 cm^3. Similar bandwidth was obtained for the 1.5 cm^3 receiving antenna, but the peak free space efficiency was only 15 %. As such, the presented antenna does not cover either the US cellular or GSM900 band totally but only narrow parts of the both bands. More tuning states are required to cover completely the both system bands, which requires more switches. This leads to even higher losses. The losses due to the PIN diodes were determined by replacing the used diodes with perfect switches (open circuit or shorting wire), and the resulting measured free space efficiency was found to be 50 % for transmitting and 20 % for receiving. It was also mentioned that the used switches exhibited nonlinearities, but no exact results were reported. As one final remark, the use of MEMS (micro-electromechanical system) switches was suggested as a future alternative, as they will have much smaller insertion loss and better linearity than the current PIN and FET switches do.

In [P7] of this thesis, the basic design principles of [P6] were adapted to a novel low-loss frequency-tuning circuit for practical mobile handset antenna (see Figure 6.1a). A tuning circuit was added to a previously published dual-band antenna element [18] for the European GSM bands to cover also the US cellular system band with the same antenna. The 4.9 cm^3 antenna was positioned on a metallized PCB having dimensions 110 mm × 40 mm, thus representing the PCB of a typical mobile phone. The tuning circuit, consisting of low-loss transmission line sections and an SPDT (single-pole, double-throw) FET switch, which had suitable characteristics for use in real mobile phones (bias voltage 3 V), was fabricated directly on the substrate of the PCB. The basic idea was to connect the first tuning line having length l_1 in turn to the second tuning line having length either $l_{2,1}$ or $l_{2,2}$ (Figure 6.1b), and thereby change the reactance loading the antenna. However, the paper introduced a problem that involves to frequency-tunable antennas positioned on a PCB with size of a typical mobile terminal; because of the strong frequency-dependency of the coupling between the feed and the antenna element, sufficient matching in both US cellular and GSM900 bands cannot be obtained by simply switching the resonant frequency of a mobile handset antenna between the two systems. This significantly complicates the design of frequency-tunable antennas for mobile handsets. In the paper, the bandwidth problem was effectively addressed by utilizing dual-resonance to provide adequate bandwidth for both systems. In the presented design, a doubly tuned resonance was used in both system bands. The results showed that an additional band of operation could be added to an existing dual-frequency antenna design with a simple tuning-circuit that causes only a small amount of additional losses (measured radiation efficiency > 72 %) and distortion (measured IIP_3 > 64 dBm and harmonic frequencies < –81 dBc). Besides, when comparing the design of [P7] with those of [30] and [32], it is claimed that the performance of the antenna presented in [P7] is much closer to the acceptable level considering a real mobile terminal.

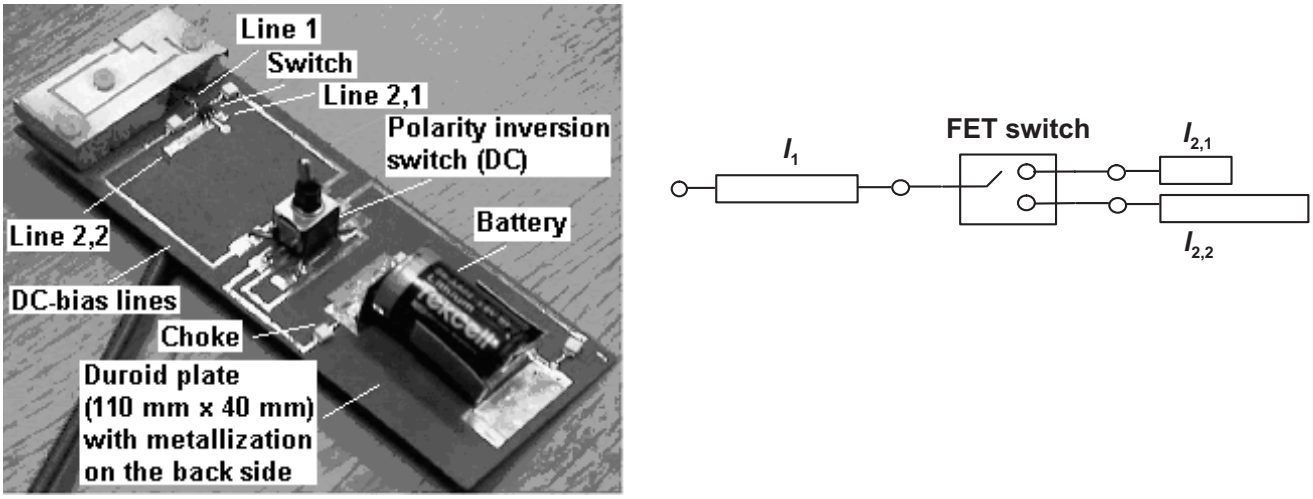

(a) (b)

Figure 6.1 *a) Photograph of the studied prototype, b) Structure of the tuning circuit.*

7 Summary of publications

[P1] On the general energy-absorption mechanism in the human tissue

In this paper, the general energy-absorption mechanism in the human tissue is investigated. The purpose is to study fundamental background to increase the understanding of this process, which has previously been somewhat unclear. The behavior of the electric fields of small antennas located near lossy dielectric half-space, which consists of several material layers, is studied by numerical simulations using a commercial FDTD-based electromagnetic solver. Two different RF sources operated at 900 MHz are used: a half-wave dipole and a patch antenna on a mobile handset chassis. The results show that the peak *SAR* is not actually related to the antenna current, as has been commonly believed. Instead, the *SAR* maximums can be explained by inspecting the quasi-static electric near fields of the antenna at the air-tissue interface and utilizing the boundary conditions.

[P2] Resonator-based analysis of the combination of mobile handset antenna and chassis

In this paper, the performance of the mobile handset antenna-chassis combination is analyzed by treating the system as a combination of the separate wavemodes of the antenna element and the chassis. A double resonator equivalent circuit model is presented and used to estimate the impedance bandwidth and the respective distribution of radiation losses with typical parameter values at 900 and 1800 MHz. The goal is to clarify the roles of different parts of the radiating system and give guidelines to control or analyze the combined performance both in the sense of radiation properties and user interaction. It is noticed, that at 900 MHz, the radiation contribution of the antenna element wavemode represents typically less than 10 % of the total radiated power. Thus, the antenna element works mainly as a matching element, which couples to the low-*Q* resonant wavemode of the chassis. At 1800 MHz, the contribution of the antenna element wavemode is larger, approximately 50 %. The results given by the theoretical study are validated by three-dimensional phone-model simulations, including calculation of the impedance bandwidth, *SAR*, and radiation efficiency in talk position. It is shown that at 900 MHz and around 10 % bandwidth, which describes a typical situation for a GSM900 mobile terminal, the contribution of the antenna element wavemode is so small that it does not have any significant effect on *SAR* or efficiency beside user. At 1800 MHz, the contribution of the chassis wavemode is found to be smaller but still significant. In addition, experimental results are presented for a prototype designed based on the model. They demonstrate that a compact non-radiating coupling element, which effectively excites the chassis wavemode, can replace a conventional self-resonant antenna element.

[P3] Bandwidth, *SAR*, and efficiency of internal mobile phone antennas

This paper presents a thorough investigation into the effects of several phone chassis -related parameters – length, width, thickness, and distance between the head and phone – on the bandwidth, efficiency in talk position, and specific absorption rate (*SAR*) characteristics of internal mobile phone antennas. The goal of this parametric approach is to provide a basis for the optimal design of antenna-chassis combination considering the performance in free space as well as beside a user. The studied antenna-chassis combinations are located beside an anatomical head model in a position of actual handset use. The effect of the user's hand is also studied with two different hand models. The main part of the study is based on FDTD simulations, but also experimental results, which support the

computationally obtained conclusions, are given. The results show the general trends of bandwidth, *SAR*, and efficiency with different chassis parameters. The results also reveal a connection between these three performance parameters: an increase in *SAR*s and a decrease in radiation efficiency occur compared to the general trend when the bandwidth reaches its maximum. This happens when the resonant frequency of the chassis equals that of the antenna.

[P4] Characteristics of half-volume DRAs with different permittivities

This paper studies experimentally the size reduction of rectangular half-volume dielectric resonator antennas. The main motivation is to determine how much the radiation efficiency decreases when downsizing the antenna by increasing the relative permittivity of the dielectric material, because this information was not available in the open literature. A set of DRAs of different permittivity material (ε_r' = 2 - 70) but of the same geometrical shape is investigated. The measurement results are given for the bandwidths, radiation patterns, gains, and radiation efficiencies of the prototypes located on large ground planes. The results show that the efficiency stays fairly high also for high values of ε_r' ($\eta_r \approx 86$ % for ε_r' = 70), which gives a good basis for the miniaturization of HV-DRAs.

[P5] Wideband dielectric resonator antenna for mobile phones

This paper describes a novel small dual-resonant dielectric resonator antenna. An antenna prototype, which is suitable for mobile terminals, is studied both theoretically and experimentally. The antenna is fed by a self-resonant meandered probe located on the surface of the dielectric dice. With this structure, a dual-resonant frequency response of the reflection coefficient and a wide impedance bandwidth is obtained. The measured impedance bandwidth ($L_{retn} \geq 6$ dB) is 28 % at $f_c = 2.36$ GHz when the antenna is positioned on a 100 mm-long chassis. The measured radiation efficiency is above 84 % over the operation band. In addition, the presented antenna is structurally simple and can be directly integrated onto a PCB.

[P6] Low-loss tuning circuits for frequency-tunable small resonant antennas

This paper deals with the minimization of power loss in the tuning circuits of frequency-tunable small resonant antennas aiming for an optimized configuration for the tuning circuit. The frequency shift and the associated power loss in certain tuning circuits are theoretically calculated based on approximate circuit models of fairly narrowband resonant antennas. The theoretical results are used to obtain design curves that facilitate the final design with an electromagnetic simulator. To support the theory, a design procedure is successfully demonstrated with two example antenna structures, for which both simulated and measured results are presented.

[P7] Frequency-tunable internal antenna for mobile phones

This paper introduces a novel low-loss frequency-tuning circuit for mobile handset antennas. The design is based on the theory presented in [P6]. The proposed tuning circuit takes into account several factors that affect the practical mobile handset antenna design, such as the biasing limitations and distortion of the switching component as well as the effect of the mobile handset -size metal plate. A handset antenna prototype that is capable of switching between the US cellular and GSM systems at 800-900 MHz frequency range is designed and measured. The designed antenna has high radiation efficiency (> 72 %) and very low distortion ($IIP_3 > 64$ dBm, harmonic frequencies < -81 dBc) in both system bands.

8 Conclusions

The entire system, which includes the antenna; the mobile terminal working in fact as part of the antenna; and the user of the terminal was considered in this thesis. The ratio between the power radiated into the free space and the antenna input power, i.e. the total efficiency of this system, formed a general concept for the studies. The ratio is affected partly by the losses owing to the user [P1]-[P3], partly by the losses in the antenna element [P4]–[P7], and partly by the losses in other mobile terminal parts.

Despite the large number of studies reporting the interaction between the mobile terminal and its user, the existing information on the general energy-absorption mechanism in the human tissue has been somewhat unclear. This thesis has made significant progress in understanding this phenomenon. It was demonstrated in the work that the peak *SAR* is not actually related to the antenna current, as has been commonly believed. Instead, the *SAR* maximums can be explained by inspecting the quasi-static electric near fields of the antenna at the air-tissue interface and utilizing the boundary conditions. It was demonstrated that for high values of the real part of tissue permittivity, such as tissue-equivalent liquid used for *SAR* compliance testing, the perpendicular electric field components are strongly attenuated at the surface. For low-permittivity tissues, like fat, the attenuation of the perpendicular components is only moderate. A simple theoretical approximation for the perpendicular electric field component in the tissue was obtained by dividing the corresponding component in free space by the real part of the relative permittivity of the tissue. The tissue surface has a similar effect on the parallel components in both cases. As *SAR* is directly proportional to the total electric field in the tissue, the *SAR* distribution caused by a certain antenna is not similar in different tissue types. The presented novel information is valuable when designing antennas with minimized user interaction, and the obtained results provide a good theoretical basis for further practical antenna designs.

Designing antennas for mobile communications devices also requires the understanding of the combined behavior of a small antenna and the metal chassis of a mobile terminal, as this has long been known to affect the antenna performance. However, this has previously been inadequately analyzed. The novel information presented in this thesis provides a clear and comprehensive picture of the interaction between a small antenna and a chassis. The studies of this thesis were made with monoblock terminals, but the results can also be applied to antennas of other terminal types, such as phones with a slider or clamshell terminals. The presented analysis is based on an approximate decomposition of the waves on the structure into two resonant wavemodes: the antenna element wavemode and the chassis wavemode. It was shown that the contribution of the chassis wavemode to the total radiated power is significant, and very large bandwidths can be realized with relatively small antenna elements by optimally utilizing the chassis wavemode. It was also demonstrated that at 900 MHz, the antenna element could actually be replaced with a practically non-resonant matching element, which was coupled to the low-Q resonant wavemode of the chassis. This idea can also be utilized in other frequency ranges. Besides the bandwidth, also the efficiency in talk position and *SAR* performance of a typical monoblock handset antenna-chassis combination were comprehensively investigated in this work. The general trends of the studied three performance parameters with different chassis parameters were shown. Also, it was demonstrated that there is a connection between these three parameters: when the resonant frequency of the chassis equals that of the antenna, the bandwidth reaches its maximum and there occur a local maximum in *SAR* values and a local minimum in radiation efficiency. Based on the results, it is concluded that the chassis currents have an important role when determining the total performance of a handset antenna-chassis combination. A thorough analysis on the behavior of the chassis currents has been presented in this thesis, but controlling those to optimize the antenna performance is an issue that should be further studied.

New approaches to realize highly efficient antenna elements for mobile terminals were also studied in this thesis. Firstly, as an alternative to commonly used microstrip-type antennas, the suitability of dielectric resonator antennas for mobile terminals was studied both theoretically and experimentally with the main attention paid to the loss characteristics. It was observed that the metal losses were not very significant even for quite small-size DRAs. Therefore, the radiation efficiency of the studied structures stayed fairly high also for antenna elements with high ε_r', which gives a good basis for the miniaturization of DRAs. Furthermore, it can be concluded that DRAs are suitable for mobile terminals, especially when very small antenna elements are needed. As an application example, a novel means to realize a high-performance dual-resonant DRA design for mobile terminals was presented in the work. Secondly, low-loss frequency-tuning circuits for small resonant antennas were systematically investigated. Equations for the theoretical calculation of the frequency shift and the associated power loss as a function of the parameters of the tuning circuit were derived in the work. Prototypes showed the validity of these equations. As the main results, general design guidelines for tuning circuits with minimized losses with respect to the achievable tuning range could be given, and an optimal configuration for the tuning circuit could be determined. In addition, the basic design principles were successfully adapted to a novel low-loss frequency-tuning circuit for practical mobile handset antennas.

This thesis provides novel and useful information for the design of mobile terminal antennas. Increasing the general understanding of the basic energy-absorption mechanism in the human tissue; a comprehensive analysis of the operation of a small antenna-terminal chassis combination; and improving the knowledge of dielectric resonator antennas and of frequency-tuning circuits of small resonant antennas both relating especially to losses in the structures can be listed as the main scientific achievements of this thesis. In addition, the work has created several technical innovations in the field of small antennas.

References

[O1] P. Vainikainen, J. Ollikainen, O. Kivekäs, and I. Kelander, *Effect of phone chassis on handset antenna performance*, Helsinki University of Technology, Radio Laboratory, Report S 240, (ISBN 951-22-4928-6), Espoo, Finland, March 2000, 13 p.

[O2] J. Ollikainen, O. Kivekäs, A. Toropainen, and P. Vainikainen, "Internal dual-band patch antenna for mobile phones," *AP2000 Millennium Conf. Antennas Propagat.*, Davos, Switzerland, 2000, paper p1111.pdf.

[O3] P. Vainikainen, J. Ollikainen, O. Kivekäs, and I. Kelander, "Performance analysis of small antennas mounted on mobile handset," *COST 259 Final Workshop - Mobile Terminal and Human Interaction*, Bergen, Norway, 2000, 8 p.

[O4] J. Juntunen, O. Kivekäs, J. Ollikainen, and P. Vainikainen, "FDTD simulation of a wide-band half volume DRA," *Proc. 5th Int. Symp. on Antennas, Propagat., and EM Theory (ISAPE 2000)*, Beijing, China, 2000, pp. 223-226.

[O5] O. Kivekäs, J. Ollikainen, J. Juntunen, and P. Vainikainen, "Comparison of DRA and patch antenna performance in handsets at 2 GHz," *Proc. 4th Eur. Personal Mobile Comm. Conf. (EPMCC 2001)*, Vienna, Austria, 2001, paper pap106.pdf.

[O6] K. Kalliola, K. Sulonen, H. Laitinen, O. Kivekäs, J. Krogerus, and P. Vainikainen, "Angular power distribution and mean effective gain of mobile antenna in different propagation environments," *IEEE Trans. Veh. Technol.*, vol. 51, no. 5, Sept. 2002, pp. 823-838.

[O7] J. Ollikainen, O. Kivekäs, L. Azzinnari, and P. Vainikainen, "Minimization of power loss in the frequency tuning circuits of small resonant antennas," *Proc. 32nd Eur. Microw. Conf. (EuMC 2002)*, Milan, Italy, 2002, pp. 433-436.

[O8] O. Kivekäs, J. Ollikainen, T. Lehtiniemi, and P. Vainikainen, "Effect of the chassis length on the bandwidth, *SAR*, and efficiency of internal mobile phone antennas," *Microw. and Opt. Technol. Lett.*, vol. 36, no. 6, March 2003, pp. 457-462.

[O9] J. Ollikainen, O. Kivekäs, C. Icheln, and P. Vainikainen, "Internal multiband handset antenna realized with an integrated matching circuit," *Proc. 12th Int. Conf. Antennas Propagat. (ICAP 2003)*, Exeter, UK, 2003, pp. 629-632.

[O10] O. Kivekäs, J. Ollikainen, T. Lehtiniemi, and P. Vainikainen, "Connection between the chassis length, bandwidth, efficiency, and *SAR* of internal mobile phone antennas," *Proc. 12th Int. Conf. Antennas Propagat. (ICAP 2003)*, Exeter, UK, 2003, pp. 735-738.

[O11] T. Laitinen, P. Vainikainen, T. Koskinen, and O. Kivekäs, "Amplitude-only vs. complex field measurements for mobile terminal antennas with a small number of measurement locations," *Proc. 20th IEEE Instrumentation Meas. Technol. Conf. (IMTC2003)*, Vail, CO, 2003, pp. 958-962.

[O12] J. Villanen, J. Ollikainen, O. Kivekäs, and P. Vainikainen, "Compact antenna structures for mobile handsets," *Proc. IEEE Veh. Technol. Conf. Fall 2003 (VTC2003-Fall)*, Orlando, FL, 2003, pp. 40-44.

[O13] Pat. US 6650295 B2, *Tunable antenna for wireless communication terminals*, Nokia Mobile Phones Ltd., Espoo, Finland, (J. Ollikainen, O. Kivekäs, and P. Vainikainen), Appl. 10/058823, 28.01.2002, granted 18.11.2003, 18 p.

[O14] Pat. FI114260, *Radiolaitteen modulaarinen kytkentärakenne ja kannettava radiolaite (Modular coupling structure for a radio device and a portable radio device)*, P. Vainikainen, J. Ollikainen, O. Kivekäs, and I. Kelander, Finland, Appl. 20002529, 17.11.2000, granted 15.09.2004, 22 p.

[O15] Pat. US 2002/0180646 A1, *Dielectric antenna*, Filtronic LK Oy, Kempele, Finland, (O. Kivekäs, J. Ollikainen, J. Juntunen, and P. Vainikainen), Appl. 10/156356, 28.05.2002, 8 p.

[1] H. A. Wheeler, "Small antennas," *IEEE Trans. Antennas Propagat.*, vol. 23, no. 4, July 1975, pp. 462-469.

[2] H. A. Wheeler, "Fundamental limitations of small antennas," *Proc. IRE*, vol. 35, Dec. 1947, pp. 1479-1488.

[3] L. J. Chu, "Physical limitations of omni-directional antennas," *J. Appl. Phys.*, vol. 19, Dec. 1948, pp. 1163-1174.

[4] H. A. Wheeler, "The radiansphere around a small antenna," *Proc. IRE*, vol. 47, no. 8, Aug. 1959, pp. 1325-1331.

[5] R. F. Harrington, "Effect of antenna size on gain, bandwidth, and efficiency," *J. of Research of the Nat. Bureau of Standards – D. Radio Propagat.*, vol. 64D, no. 1, Jan.-Feb. 1960, pp. 1-12.

[6] R. C. Hansen, "Fundamental limitations in antennas," *Proc. IEEE*, vol. 69, no. 2, Feb. 1981, pp. 170-182.

[7] H. A Wheeler, "The wide-band matching area for a small antenna," *IEEE Trans. Antennas Propagat.*, vol. 31, no. 2, March 1983, pp. 364-367.

[8] J. McLean, "A re-examination of the fundamental limits on the radiation Q of electrically small antennas," *IEEE Trans. Antennas Propagat.*, vol. 44, no. 5, May 1996, pp. 672-676.

[9] R. Vaughan and J. Bach Andersen, *Channels, propagation, and antennas for mobile communications*, The Institution of Electrical Engineers, Cornwall, UK, 2003, 753 p.

[10] O. Lehmus, *Miniaturization methods of handset antennas*, Master's Thesis, Helsinki University of Technology, Radio Laboratory, Espoo, Finland, Feb. 1999, 99 p.

[11] J. Toftgård, S. N. Hornstleht, and J. B. Andersen, "Effects on portable antennas of the presence of a person," *IEEE Trans. Antennas Propagat.*, vol. 41, no. 6, June 1993, pp.739-746.

[12] M. A. Jensen and Y. Rahmat-Samii, "EM interaction of handset antennas and a human in personal communications," *Proc. IEEE*, vol. 83, no. 1, Jan. 1995, pp. 7-17.

[13] J. T. Rowley and R. B. Waterhouse, "Performance of shorted microstrip patch antennas for mobile communications handsets at 1800 MHz," *IEEE Trans. Antennas Propagat.*, vol. 47, no. 5, May 1999, pp. 815-822.

[14] D. Manteuffel, A. Bahr, D. Heberling, and I. Wolff, "Design considerations for integrated mobile phone antennas," *Proc. 11th Int. Conf. Antennas Propagat. (ICAP 2001)*, Manchester, UK, 2001, pp. 252-256.

[15] Z. D. Liu, P. S. Hall, and D. Wake, "Dual-frequency planar inverted-F antenna," *IEEE Trans. Antennas Propagat.*, vol. 45, no. 10, Oct. 1997, pp. 1451-1458.

[16] C. R. Rowell and R. D. Murch, "Compact PIFA suitable for dual-frequency 900/1800-MHz operation," *IEEE Trans. Antennas Propagat.*, vol. 46, no. 4, Apr. 1998, pp. 596-598.

[17] P. Song, P. S. Hall, H. Ghafouri-Shiraz, and D. Wake, "Triple band planar inverted F antennas for handheld devices," *Electron. Lett.*, vol. 36, no., 2, Jan. 2000, pp. 112-114.

[18] S. Tarvas and A. Isohätälä, ”An internal dual-band mobile phone antenna,” *IEEE Antennas Propagat. Int. Symp. Dig. (AP-S 2000)*, Salt Lake City, UT, 2000, pp. 266-269.

[19] M. Martinez-Vázquez and O. Litschke, “Quadband antenna for handheld personal communications devices,” *IEEE Antennas Propagat. Int. Symp. Dig. (AP-S 2003)*, Columbus, OH, 2003, pp. 455-458.

[20] T.-S. Yung, T.-H. Chang, W.-Z. Wu, and J.-F. Kiang, “Dual-band dielectric resonant antenna,” *IEEE Antennas Propagat. Int. Symp. Dig. (AP-S 2004)*, Monterey, CA, 2004, pp.1351-1354.

[21] A. Buerkle, K. Sarabandi, and H. Mosallaei, “A novel approach to enhance the bandwidth of miniaturized dielectric resonator antennas,” *IEEE Antennas Propagat. Int. Symp. Dig. (AP-S 2004)*, Monterey, CA, 2004, pp. 1359-1362.

[22] G. Bit-Babik, C. Di Nallo, and A. Faraone, “Multimode dielectric resonator antenna of very high permittivity,” *IEEE Antennas Propagat. Int. Symp. Dig. (AP-S 2004)*, Monterey, CA, 2004, pp. 1383-1386.

[23] J. Ollikainen, *Design and implementation techniques of wideband mobile communications antennas*, Doctoral Thesis, Helsinki University of Technology, Radio Laboratory, Espoo, Finland, Nov. 2004.

[24] J. Fuhl, P. Nowak, and E. Bonek, “Improved internal antenna for hand-held terminals,” *Electron. Lett.*, vol. 30, no. 22, Oct. 1994, pp. 1816-1818.

[25] K. L. Virga and Y. A. Rahmat-Samii, “Low-profile enhanced bandwidth PIFA antennas for wireless communications packaging,” *IEEE Trans. Antennas Propagat.*, vol. 45, no. 10, Oct. 1997, pp. 1879-1888.

[26] J. Ollikainen, M. Fischer, and P. Vainikainen, “Thin dual-resonant stacked shorted patch antenna for mobile communications,” *Electron. Lett.*, vol. 35, no. 6, March 1999, pp. 437-438.

[27] H. F. Pues and A. R. Van de Capelle, “An impedance matching technique for increasing the bandwidth of microstrip antennas,” *IEEE Trans. Antennas Propagat.*, vol. 37, no. 11, Nov. 1989, pp. 1345-1354.

[28] P. Ciais, R. Staraj, G. Kossiavas, and C. Luxey, “Compact internal multiband antenna for mobile phone and WLAN standards,” *Electron. Lett.*, vol. 40, no. 15, July 2004, pp. 920- 921.

[29] P. Bhartia and I. J. Bahl, “Frequency agile microstrip antennas,” *Microw. J.*, vol. 25, Oct. 1982, pp. 67-70.

[30] J.-P. Louhos and I. Pankinaho, “Electrical tuning of integrated mobile phone antennas,” *Proc. 1999 Antenna Applications Symposium*, Monticello, IL, 1999, pp. 69-97.

[31] R. B. Waterhouse and N. V. Shuley, “Full characterization of varactor-loaded, probe-fed, rectangular microstrip patch antennas,” *IEE Proc.-Microw. Antennas Propagat.*, vol. 141, no. 5, Oct. 1994, pp. 367-373.

[32] J. T. Aberle, S.-H. Oh, D. T. Auckland, and S. D. Rogers, “Reconfigurable antennas for portable wireless devices,” *IEEE Antennas Propagat. Magazine*, vol. 45, no. 6, Dec. 2003, pp. 148-154.

[33] P. S. Hall, S. D. Kapoulas, R. Chauhan, and C. Kalialakis, “Microstrip patch antenna with integrated adaptive tuning,” *Proc. 10th Int. Conf. Antennas Propagat. (ICAP 1997)*, Edinburgh, UK, 1997, pp. 506-509.

[34] C. Kalialakis, P. Gardner, and P. S. Hall, “Harmonic radiation from varactor-loaded microstrip antennas,” *Proc. 31st Eur. Microw. Conf. (EuMC2001)*, London, UK, 2001, pp. 133-136.

[35] K. R. Boyle, “Mobile phone antenna performance in the presence of people and phantoms,” *IEE Technical Seminar Antenna Meas. and SAR (AMS 2002)*, Loughborough University, UK, 2002, 4 p.

[36] K. R. Boyle, “The performance of GSM 900 antennas in the presence of people and phantoms,” *Proc. 12th Int. Conf. Antennas Propagat. (ICAP 2003)*, Exeter, UK, 2003, pp. 35-38.

[37] M. Burkhardt and N. Kuster, “Review of exposure assessment for handheld mobile communications devices and antenna studies for optimised performance,” Chapter 34 in *The Review of Radio Science 1996-1999*, W. R. Stone (Editor), Oxford University Press, New York, NY, 1999.

[38] P. Bernardi, M. Cavagnaro, S. Pisa, and E. Piuzzi, “Specific absorption rate and temperature increases in the head of a cellular-phone user,” *IEEE Trans. Microw. Theory Tech.*, vol. 48, no. 7, July 2000, pp. 1118-1126.

[39] P. J. Dimbylow and S. M. Mann, “SAR calculations in an anatomically realistic model of the head for mobile communication transceivers at 900 MHz and 1.8 GHz,” *Physics in Medicine and Biology*, vol. 39, no. 10, Oct. 1994, pp. 1537-1553.

[40] M. G. Douglas, M. Okoniewski, and M. Stuchly, “A planar diversity antenna for handheld PCS devices,” *IEEE Trans. Veh. Technol*., vol. 47, no. 3, Aug. 1998, pp. 747-754.

[41] J. Graffin, N. Rots, and G. F. Pedersen, “Radiations phantom for handheld phones,” *Proc. IEEE Veh. Technol. Conf. Fall 2000 (VTC2000- Fall)*, Boston, MA, 2000, pp. 853-866.

[42] T. Schmid, O. Egger, and N. Kuster, “Automated E-field scanning system for dosimetric assessments,” *IEEE Trans. Microw. Theory Techn.*, vol. 44, no. 1, Jan. 1996, pp. 105-113.

[43] N. Kuster, R. Kästle, and T. Schmid, ”Dosimetric evaluation of handheld mobile communications equipment with known precision,” *IEICE Trans. Commun.*, vol. E80-B, May 1997, pp. 645-652.

[44] Q. Yu, O.-P. Gandhi, M. Aronsson, and D. Wu, “An automated SAR measurement system for compliance testing of personal wireless devices,” *IEEE Trans. Electromagn. Compat.*, vol. 41, no. 3, Aug. 1999, pp. 234-245.

[45] M. Okoniewski, “Advances in computational dosimetry,” *13th Int. Conf. Microw., Radar and Wireless Comm. (MIKON-2000)*, Wroclaw, Poland, 2000, pp. 82-93.

[46] Federal Communications Commission (FCC), Office of Engineering and Technology (OET), *Evaluating Compliance with the FCC Guidelines for Human Exposure to Radiofrequency Electromagnetic Fields, Additional Information for Evaluating Compliance of Mobile and Portable Devices with FCC limits for Human Exposure to Radiofrequency Emissions*, Supplement C to OET Bulletin 65, June 2001, 57 p.

[47] The Council of the European Union, “Council recommendation on 12 July 1999 on the limitation of exposure of the general public to electromagnetic fields (0 Hz to 300 GHz),” 1999/519/EC, *Official Journal of the European Communities*, L 199, July 1999, pp. 59-70.

[48] ANSI / IEEE Std C95.1, 1999 Edition, *IEEE Standard for Safety Levels with Respect to Human Exposure to Radio Frequency Electromagnetic Fields, 3 kHz to 300 GHz*, April 1999, 73 p.

[49] International Commission on Non-Ionizing Radiation Protection (ICNIRP), “Guidelines for limiting exposure to time-varying electric, magnetic, and electromagnetic fields (up to 300 GHz),” *Health Physics*, vol. 74, no. 4, April 1998, pp. 494-522.

[50] A. C. Metaxas and R. J. Meredith, *Industrial Microwave Heating*, Peter Peregrinus Ltd, Exeter, UK, 1983, 357 p.

[51] N. Kuster and Q. Balzano, "Energy absorption mechanism by biological bodies in the near field of dipole antennas above 300 MHz," *IEEE Trans. Veh. Technol.*, vol. 41, pp. 17-23, Feb. 1992.

[52] H.-R. Chuang, "Numerical computation of fat layer effects on microwave near-field radiation to the abdomen of a full-scale human body model," *IEEE Trans. Microw. Theory Tech.*, vol. 45, pp. 118-125, Jan. 1997.

[53] E. Nyfors and P. Vainikainen, *Industrial Microwave Sensors*, Artech House, Norwood, MA, 1989, 351 p.

[54] R. E. Harrington, *Time-Harmonic Electromagnetic Fields*, McGraw-Hill, New York, NY, 1961, 480 p.

[55] T. Taga and K. Tsunekawa, "Performance analysis of a built-in planar inverted F antenna for 800 MHz band portable radio units," *IEEE J. Select. Areas Commun.*, vol. 5, no. 5, June 1987, pp. 921-929.

[56] K. Sato, K. Matsumoto, K. Fujimoto, and K. Hirasawa, "Characteristics of a planar inverted-F antenna on a rectangular conducting body," *Electron. Commun. in Japan*, pt. 1, vol. 72, 1989, pp. 43-51.

[57] E. Antonino-Daviu, M. Cabedo-Fabrés, M. Ferrando-Bataller, and J. I. Herranz-Herruzo, "Analysis of the coupled chassis-antenna modes in mobile handsets," *IEEE Antennas Propagat. Int. Symp. Dig. (AP-S 2004)*, Monterey, CA, 2004, pp. 2751-2754.

[58] E. Antonino-Daviu, M. Cabedo-Fabrés, M. Ferrando-Bataller, and A. Valero-Nogueira, "Design of small antennas for mobile terminals," *Proc. 6th COST 284*, Barcelona, Spain, 2004, 4 p.

[59] R. F. Harrington and J. R. Mautz, "Theory of characteristic modes for conducting bodies," *IEEE Trans. Antennas Propagat.*, vol. 19, no. 5, Sept. 1971, pp. 622-628.

[60] D.-U. Sim. J.-I. Moon, and S.-O. Park, "An internal triple-band antenna for PCS/IMT-2000/Bluetooth applications," *IEEE Antennas Wireless Propagat. Lett.*, vol. 3, 2004, pp. 23-25.

[61] D. Manteuffel, A. Bahr, and I. Wolff, "Investigation on integrated antennas for GSM mobile phones," *AP2000 Millennium Conf. Antennas Propagat.*, Davos, Switzerland, 2000, paper p0351.pdf.

[62] D. Manteuffel, A. Bahr, D. Heberling, and I. Wolff, "Design considerations for integrated mobile phone antennas," *Proc. 11th Int. Conf. Antennas Propagat. (ICAP 2001)*, Manchester, UK, 2001, pp. 252-256.

[63] A. T. Arkko and E. A. Lehtola, "Simulated impedance bandwidths, gains, radiation patterns and *SAR* values of a helical and a PIFA antenna on top of different ground planes," *Proc. 11th Int. Conf. Antennas Propagat. (ICAP 2001)*, Manchester, UK, 2001, pp. 651-654.

[64] R. Hossa, A. Byndas, and M. E. Bialkowski, "Improvement of compact terminal antenna performance by incorporating open-end slots in ground plane," *IEEE Microw. Wireless Components Lett.*, vol. 14, no. 6, June 2004, pp. 283-285.

[65] M. F. Abedin and M. Ali, “Modifying the ground plane and its effect on planar inverted-F antennas (PIFAs) for mobile phone handsets,” *IEEE Antennas Wireless Propagat. Lett.*, vol. 2, 2003, pp. 226-229.

[66] M. Geissler, D. Heberling, and I. Wolff, “Properties of integrated handset antennas,” *AP2000 Millennium Conf. Antennas Propagat.*, Davos, Switzerland, 2000, paper p0526.pdf.

[67] J. Villanen, *Compact antenna structure for mobile handsets*, Master’s Thesis, Helsinki University of Technology, Espoo, Finland, Feb. 2003, 84 p.

[68] D. Manteuffel, A. Bahr, P. Waldow, and I. Wolff, “Numerical analysis of absorption mechanisms for mobile phones with integrated multiband antennas,” *IEEE Antennas Propagat. Int. Symp. Dig. (AP-S 2001)*, Boston, MA, 2001, pp. 82-85.

[69] O. Kivekäs, *Small mobile terminal antennas with low user interaction*, Licentiate thesis, Helsinki University of Technology, Radio Laboratory, Espoo, Finland, Aug. 2001, 105 p.

[70] P. Panayi, M. Al-Nuaimi, and L. P. Ivrissimtzis, ”Near/far field and SAR of mobile communication antennas,” *AP2000 Millennium Conf. Antennas Propagat.*, Davos, Switzerland, 2000, paper p0351.pdf.

[71] M. Sager, M. Forcucci, and T. Kristensen, “A novel technique to increase the realized efficiency of a mobile phone antenna place beside a head-phantom,” *IEEE Antennas Propagat. Int. Symp. Dig. (AP-S 2003)*, Columbus, OH, 2003, pp. 1013-1016.

[72] D. Manteuffel, “Design of multiband antennas for the integration in mobile phones with optimized SAR,” *IEEE Antennas Propagat. Int. Symp. Dig. (AP-S 2003)*, Columbus, OH, 2003, pp. 66-69.

[73] M. Okoniewski and M. Stuchly, “A study of the handset antenna and human body interaction,” *IEEE Trans. Microw. Theory Techn.*, vol. 44, no. 10, Oct. 1996, pp. 1855-1864.

[74] A. Schiavoni, P. Bertotto, G. Richiardi, and P. Bielli, “SAR generated by commercial cellular phones – phone modeling, head modeling, and measurements,” *IEEE Trans. Microw. Theory Techn.*, vol. 48, no. 11, Nov. 2000, pp. 2064-2071.

[75] D. Kajfez and P. Guillon, (Eds.), *Dielectric Resonators*, Artech House, Dedham, MA, 1986, 539 p.

[76] S. A. Long, M. W. Allister, and L. C. Shen, “The resonant cylindrical dielectric cavity antenna,” *IEEE Trans. Antennas Propagat.*, vol. 31, no. 3, May 1983, pp. 406-412.

[77] R. K. Mongia and P. Bhartia, “Dielectric resonator antennas – a review and general design relations for resonant frequency and bandwidth,” *Int. J. of Microw. and Millim.-Wave Computer-Aided Eng.*, vol. 4, no. 3, 1994, pp. 230-247.

[78] M. K. Tam and R. D. Murch, “Half volume dielectric resonator antenna designs,” *Electron. Lett.*, vol. 33, no. 23, Nov. 1997, pp. 1914-1916.

[79] R. E. Collin, *Antennas and Radiowave Propagation*, McGraw-Hill, Singapore, 1985, 508 p.

[80] R. K. Mongia and A. Ittipiboon, “Theoretical and experimental investigations on rectangular dielectric resonator antennas,” *IEEE Trans. Antennas Propagat.*, vol. 45, no. 9, Sept. 1997, pp. 1348-1356.

[81] J. Moon and S. Park, “Dielectric resonator antenna for dual-band PCS/IMT-2000,” *Electron. Lett.*, vol. 36, no. 12, June 2000, pp. 1002-1003.

[82] K. P. Esselle, “A dielectric-resonator-on-patch (DROP) antenna for broadband wireless applications: concept and results,” *IEEE Antennas Propagat. Int. Symp. Dig. (AP-S 2001),* Boston, MA, July 2001, pp. 22-25.

[83] M. T. Lee, K. M. Luk, K. W. Leung, and M. K. Leung, “A small dielectric resonator antenna,” *IEEE Trans. Antennas Propagat*., vol. 50, no. 10, Oct. 2002, pp. 1485-1487.

[84] D. Gray and T. Watanabe, “Three orthogonal polarization DRA-monopole ensemble,” *Electron. Lett.*, vol. 39, no. 10, May 2003, pp. 766-767.

[85] M. T. K. Tam and R. D. Murch, “Compact circular sector and annular sector dielectric resonator antennas,” *IEEE Trans. Antennas Propagat.*, vol. 47, no. 5, May 1999, pp. 837-842.

[86] D. Cormos, A. Laisne, R. Gillard, F. Le Bolzer, and C. Nicolas, ”Compact dielectric resonator antenna for WLAN applications,” *Electron. Lett.*, vol. 39, no. 7, April 2003, pp. 588-590.

[87] P. K. Panayi, M. O. Al-Nuaimi, and L. P. Ivrissimtzis, ”Tuning techniques for planar inverted F-antenna,” *Electron. Lett.*, vol. 37, no. 16, Aug. 2001, pp. 1003-1004.

[88] F. Yang and Y. Rahmat-Samii, “Patch antenna with switchable slot (PASS): dual-frequency operation,” *Microw. and Opt. Tech. Lett.*, vol. 31, no. 3, Nov. 2001, pp. 165-168.

[89] J. M. Carrère, R. Staraj, and G. Kossiavas, “Small frequency agile antennas,” *Electron. Lett.*, vol. 37, no. 12, June 2001, pp. 728-729.

[90] H. Okabe and K. Takei, “Tunable antenna system for 1.9-GHz PCS handsets,” *IEEE Antennas Propagat. Int. Symp. Dig. (AP-S 2001),* Boston, MA, 2001, pp. 166-169.

[91] N. C. Karmakar, P. Hendro, and L. S. Firmansyah, “Shorting strap tunable single feed dual-band PIFA,” *IEEE Microw. Wireless Components Lett.,* vol. 13, no. 1, Jan. 2003, pp. 13-15.